Extended Successive Convex Approximation for Phase Retrieval with Dictionary Learning

Tianyi Liu (刘添翼), Andreas M. Tillmann, Yang Yang (杨阳), Yonina C. Eldar, and Marius Pesavento

***Abstract*—Phase retrieval aims at reconstructing unknown signals from magnitude measurements of linear mixtures. In this paper, we consider the phase retrieval with dictionary learning problem, which includes an additional prior information that the measured signal admits a sparse representation over an unknown dictionary. The task is to jointly estimate the dictionary and the sparse representation from magnitude-only measurements. To this end, we study two complementary formulations and develop efficient parallel algorithms by extending the successive convex approximation framework using a smooth majorization. The first algorithm is termed *compact-SCAphase* and is preferable in the case of less diverse mixture models. It employs a compact formulation that avoids the use of auxiliary variables. The proposed algorithm is highly scalable and has reduced parameter tuning cost. The second algorithm, referred to as *SCAphase*, uses auxiliary variables and is favorable in the case of highly diverse mixture models. It also renders simple incorporation of additional side constraints. The performance of both methods is evaluated when applied to blind sparse channel estimation from subband magnitude measurements in a multi-antenna random access network. Simulation results demonstrate the efficiency of the proposed techniques compared to state-of-the-art methods.**

***Index Terms*—phase retrieval, dictionary learning, successive convex approximation, majorization-minimization, nonconvex optimization, nonsmooth optimization**

I. INTRODUCTION

PHASE retrieval refers to the problem of recovering an unknown complex-valued signal from the (squared) magnitude of linear measurements corrupted by additive noise. It has received considerable attention in various applications such as diffraction imaging [2], [3], astronomy [4], and X-ray crystallography [5], where the measurement of intensity (squared magnitude) is usually much easier than that of phase. In some other applications, including non-coherent direction-of-arrival estimation [6], the loss of phase information is caused by imperfect phase synchronization.

In recent years, numerous phase retrieval approaches have been developed, which can be principally classified as nonconvex and convex ones. In the nonconvex optimization methods, the recovery problem is formulated as a nonconvex least-squares (LS) problem. Stationary points of the nonconvex

T. Liu and M. Pesavento are with TU Darmstadt, 64283 Darmstadt, Germany (e-mail: tliu@nt.tu-darmstadt.de; pesavento@nt.tu-darmstadt.de).

A. M. Tillmann is with TU Braunschweig, 38106 Braunschweig, Germany (e-mail: a.tillmann@tu-braunschweig.de).

Y. Yang is with Fraunhofer Institute for Industrial Mathematics, 67663 Kaiserslautern, Germany, and the Fraunhofer Center Machine Learning (e-mail: yang.yang@itwm.fraunhofer.de).

Y. C. Eldar is with Weizmann Institute of Science, Rehovot 7610001, Israel(e-mail: yonina.eldar@weizmann.ac.il).

Part of this work is accepted for publication at IEEE ICASSP 2021 [1].

formulation can then be obtained by classic continuous optimization algorithms such as alternating projections [4], [7], gradient descent [8]–[10], and alternating direction method of multipliers (ADMM) [11], [12]. A popular class of convex optimization approaches employs semidefinite relaxation [13]–[16], which lifts the problem to a higher dimension and is, hence, computationally prohibitive for large-scale problems. Recently, some non-lifting convex optimization approaches have been developed based on solving a basis pursuit problem in the dual domain, including PhaseMax [17] and PhaseEqual [18]. A comprehensive review of recent advances in phase retrieval from a numerical perspective is presented in [19].

On the other hand, additional prior information on the unknown signal, such as sparsity, can be used to improve uniqueness and stability of the reconstruction [20]. Most of the aforementioned phase retrieval approaches have been adapted to recovering signals that are sparse either in the standard basis or in a known dictionary [18], [21]–[27]. The GESPAR algorithm is based on the damped Gauss-Newton method [21]. Majorization-Minimization (MM) algorithms are devised in [23]. In [24], the Truncated Amplitude Flow (TAF) method is extended to recovering sparse signals. The STELA algorithm proposed in [27] is based on the successive convex approximation (SCA) and can be parallelized.

Phase retrieval was generalized in [28] to jointly learning an unknown dictionary and a sparse representation. To tackle the joint estimation problem, the authors propose a regularized nonconvex LS formulation with squared magnitude measurements and develop an alternating minimization algorithm termed DOLPHIn. In [23], the authors apply a similar regularized LS formulation to magnitude measurements and solve it by an algorithm based on block successive upper-bound minimization (BSUM), named SC-PRIME. There, it is shown by both theoretical justification and numerical results that the reconstruction from magnitude measurement outperforms that from intensity measurements. However, the use of auxiliary variables in both aforementioned methods depresses the scalability and, more notably, increases the number of hyperparameters that require tuning. Moreover, neither of the two methods can take full benefit of modern parallel hardware architectures. In addition, SC-PRIME often suffers from slow convergence due to the loose approximation used by BSUM.

The SCA framework [29] possesses the advantage of parallelism. However, it can only be applied to a composite problem with a smooth loss function and a convex but not necessarily smooth regularization. In this paper, to address the phase retrieval with dictionary learning problem given the magnitude measurements, which is formulated as a nonsmooth

and nonconvex LS problem, we extend the SCA framework using a smooth majorization. The extended framework inherits the parallel nature of the original SCA framework. Two efficient parallel algorithms for the phase retrieval and dictionary learning problem are proposed by applying the extended SCA framework to two complementary formulations, respectively. Specifically, we first study a compact formulation that avoids the auxiliary variables and the proposed extended-SCA algorithm is termed *compact-SCAphase*. Then, another algorithm based on the extended SCA framework is proposed for the conventional formulation with auxiliary variables, which is referred to as *SCAphase* (Successive Convex Approximation for phase retrieval with dictionary learning). The performance of the proposed algorithms is evaluated when applied to blind sparse channel estimation from subband magnitude measurements in a multi-antenna random access network. Simulation results on synthetic data show the fast convergence of the proposed algorithms compared to the state-of-the-art method SC-PRIME [23]. In the case with less diverse linear mixing models, compact-SCAphase is more competitive than SCAphase in terms of both computational complexity and parameter tuning cost. However, for highly diverse linear measurement operators, the computational complexity of compact-SCAphase dramatically grows, compared to SCAphase. To summarize, the main contributions of this paper are:

- We introduce an extension of SCA framework for the phase retrieval with dictionary learning problem. Two efficient parallel algorithms are proposed by applying the extended SCA framework to two complementary formulations, respectively.
- The convergence of the extended SCA framework is established based on a generalized concept of stationarity. Our novel convergence analysis also be used to establish the convergence of SC-PRIME [23].
- To reduce the overall computational complexity of compact-SCAphase, an efficient procedure based on rational approximation is devised for solving the ℓ_2-norm constrained LS subproblems.

The paper is organized as follows. In Section II, we introduce the signal model and provide two different mathematical formulations with and without auxiliary variables, respectively, for the phase retrieval with dictionary learning problem. The proposed algorithms for both formulations are described in Section III and IV, respectively. In Section V, we establish the convergence of the proposed algorithms and analyze the computational complexity in comparison to SC-PRIME. Simulation results on synthetic data are presented and discussed in Section VI and conclusions are drawn in Section VII.

II. NOTATION AND PROBLEM FORMULATION

A. Notation

We use x, $\mathbf{x}$ and $\mathbf{X}$ to denote a scalar, column vector and matrix, respectively; $\mathbb{R}$ and $\mathbb{C}$ are the set of real and complex numbers. The letter j is reserved to denote the imaginary unit. For any $x\in\mathbb{C}$, $|x|$ denotes its magnitude, $\arg(x)$ its phase, $\bar{x}$ its complex conjugate, and $\Re(x)$ its real part. The operator $\mathcal{S}_\lambda(x)=\max\{0,|x|-\lambda\}\cdot e^{\mathrm{j}\arg(x)}$ is the soft-thresholding operator.

The superscripts $(\cdot)^\mathrm{T},(\cdot)^\mathrm{H},(\cdot)^{-1}$, and $(\cdot)^\dagger$ denote the transpose, Hermitian transpose, inverse and pseudoinverse, respectively. For a matrix $\mathbf{X}\in\mathbb{C}^{M\times N}$, x_{kl} is its (k,l)-th element, $\mathbf{x}_l$ its l-th column, $\mathbf{x}_{k:}^\mathrm{T}$ its k-th row, $\mathrm{vec}(\mathbf{X})=[\mathbf{x}_1^\mathrm{T},...,\mathbf{x}_N^\mathrm{T}]^\mathrm{T}\in\mathbb{C}^{MN}$ its vectorized form, and $\|\mathbf{X}\|_1=\sum_{k,l}|x_{kl}|$ its element-wise ℓ_1-norm. The trace operator is written as $\mathrm{tr}(\cdot)$ and $\|\cdot\|_\mathrm{F}$ is the Frobenius norm. For a vector $\mathbf{x}$, the k-th entry is x_k. Also, the k-th entry of a vector $\mathbf{x}_l$ that itself carries a subscript will be denoted by x_{kl}. $\odot$ and $\otimes$ denote the Hadamard and Kronecker products, respectively; $\mathbf{0}$ is a matrix with all elements 0.

For a linear operator $\mathcal{F}(\cdot)$, $\mathcal{F}^*(\cdot)$ is its adjoint operator. For a real-valued function $f(\mathbf{X})$ with real arguments $\mathbf{X}\in\mathbb{R}^{M\times N}$, $\nabla_\mathbf{X} f(\mathbf{X})$ is the gradient with respect to $\mathbf{X}$, which is an $M\times N$ matrix with the (k,l)-th entry being $\frac{\partial}{\partial x_{kl}}f(\mathbf{X})$, and $\nabla_{\mathrm{vec}(\mathbf{X})}f(\mathbf{X})$ denotes the vectorized form of the gradient. The Hessian matrix defined with the vectorized arguments is denoted by $\nabla^2_{\mathrm{vec}(\mathbf{X})}f(\mathbf{X})$, which is an $MN\times MN$ matrix with the (mn,kl)-th entry being $\frac{\partial^2}{\partial x_{mn}\partial x_{kl}}f(\mathbf{X})$. Also, $\nabla^2_{x_{kl}}f(\mathbf{X})=[\nabla^2_{\mathrm{vec}(\mathbf{X})}f(\mathbf{X})]_{kl,kl}$ denotes the diagonal entry corresponding to the argument x_{kl} in the Hessian matrix. As for complex arguments $\mathbf{X}\in\mathbb{C}^{M\times N}$, we define the entries of gradient and Hessian matrix as follows: $[\nabla_\mathbf{X} f(\mathbf{X})]_{k,l}=2\frac{\partial}{\partial\bar{x}_{kl}}f(\mathbf{X})$ and $[\nabla^2_{\mathrm{vec}(\mathbf{X})}f(\mathbf{X})]_{mn,kl}=2\frac{\partial^2}{\partial\bar{x}_{mn}\partial x_{kl}}f(\mathbf{X})$, where $\frac{\partial}{\partial x}$ and $\frac{\partial}{\partial\bar{x}}$ are the Wirtinger derivative operators [30]. Thus, for both real and complex arguments, a real-valued quadratic function $f(\mathbf{X})$ can be written as a second-order Taylor series in a unified form

$$f(\mathbf{X})=f(\mathbf{X}_0)+\Re\Big(\mathrm{tr}\big((\mathbf{X}-\mathbf{X}_0)^\mathrm{H}\nabla_\mathbf{X} f(\mathbf{X}_0)\big)\Big)$$
$$+\frac{1}{2}(\mathrm{vec}(\Delta\mathbf{X}))^\mathrm{H}\nabla^2_{\mathrm{vec}(\mathbf{X})}f(\mathbf{X}_0)(\mathrm{vec}(\Delta\mathbf{X})),$$

where $\Delta\mathbf{X}=\mathbf{X}-\mathbf{X}_0$ and $\mathbf{X}_0$ is any given point.

B. Problem Formulation

We consider the following nonlinear system. For an input signal $\mathbf{X}\in\mathbb{K}^{N\times I}$, $\mathbb{K}\in\{\mathbb{R},\mathbb{C}\}$, the following noise-corrupted magnitude-only measurements are observed:

$$\mathbf{Y}=|\mathcal{F}(\mathbf{X})|+\mathbf{N}, \tag{1}$$

where $\mathcal{F}:\mathbb{C}^{N\times I}\to\mathbb{C}^{M_1\times M_2}$ is a linear operator, $\mathbf{N}$ is a real matrix whose entries represent noise, and the absolute value operation $|\cdot|$ is applied element-wise. We remark that a general linear mixing operator $\mathcal{F}(\cdot)$ can be expressed equivalently as

$$\mathrm{vec}\big(\mathcal{F}(\mathbf{X})\big)=\mathbf{F}\cdot\mathrm{vec}(\mathbf{X}), \tag{2}$$

with vectorized variables and a suitable matrix $\mathbf{F}\in\mathbb{C}^{M_1M_2\times NI}$, which we will also use in this paper. The negative entries of $\mathbf{Y}$ resulting from noise will be set to 0. Moreover, each column $\mathbf{x}_i$ in signal $\mathbf{X}$ is assumed to admit a sparse representation over an unknown dictionary $\mathbf{D}\in\mathbb{K}^{N\times P}$, i.e., $\mathbf{x}_i=\mathbf{D}\mathbf{z}_i$ with a sparse code vector $\mathbf{z}_i\in\mathbb{K}^P$. Let $\mathbf{Z}=[\mathbf{z}_1,...,\mathbf{z}_I]$ be the matrix containing the sparse code vectors as columns. Our objective is to jointly learn the dictionary $\mathbf{D}$ and the sparse codes $\mathbf{Z}$ so as to minimize the (LS) reconstruction error.

To this end, we solve the following compact formulation for phase retrieval with dictionary learning (cPRDL) problem:

$$\text{cPRDL:}\quad \min_{\mathbf{D}\in\mathcal{D},\mathbf{Z}} \quad \frac{1}{2}\|\mathbf{Y}-|\mathcal{F}(\mathbf{D}\mathbf{Z})|\|_\mathrm{F}^2+\lambda\|\mathbf{Z}\|_1. \tag{3}$$

The first term evaluates the data fidelity by the LS criterion, which is nonsmooth and nonconvex due to the element-wise

absolute value operation. The second term promotes sparsity in $\mathbf{Z}$, where $\lambda \geq 0$ is a regularization parameter. To avoid scaling ambiguities, we restrict $\mathbf{D}$ to be in the convex set $\mathcal{D}=\{\mathbf{D}\in \mathbb{K}^{N\times P}\|\|\mathbf{d}_p\|_2\leq 1,\forall p=1,...,P\}$. Each column $\mathbf{d}_p$ is called an atom and the number of atoms is assumed to be less than the number of columns in $\mathbf{X}$, i.e., $P<I$. Otherwise, each column $\mathbf{x}_i$ can be trivially represented by a vector $\mathbf{z}_i$ with one nonzero entry by including $\mathbf{x}_i/\|\mathbf{x}_i\|_2$ as an atom.

An alternative formulation for phase retrieval with dictionary learning (PRDL), which we will also consider in this paper, is obtained by replacing $\mathbf{DZ}$ in the data fidelity term by an auxiliary variable $\mathbf{X}$:

$$\text{PRDL:}\ \min_{\mathbf{X},\mathbf{D}\in\mathcal{D},\mathbf{Z}}\tfrac{1}{2}\|\mathbf{Y}-|\mathcal{F}(\mathbf{X})|\|_{\text{F}}^2+\tfrac{\mu}{2}\|\mathbf{X}-\mathbf{DZ}\|_{\text{F}}^2+\rho\|\mathbf{Z}\|_1. \quad (4)$$

The additional second term measures how well the signal $\mathbf{X}$ can be approximated by the sparse representation $\mathbf{DZ}$. Two regularization parameters $\mu,\rho\geq 0$ are used to balance the data fidelity, the approximation quality, and the code sparsity. Likewise, $P<I$ is required to avoid trivial dictionaries.

The formulation (4) was first proposed in [28], however, with the intensity measurements $\widetilde{\mathbf{Y}}=|\mathcal{F}(\mathbf{X})|^2+\mathbf{N}$, which results in another smooth data fidelity term: $\tfrac{1}{4}\|\widetilde{\mathbf{Y}}-|\mathcal{F}(\mathbf{X})|^2\|_{\text{F}}^2$. In [23], the authors have shown that, for the intensity measurements $\widetilde{\mathbf{Y}}$, it is also beneficial, in the high SNR regime, to use formulation (4) with the modulus information $\sqrt{\widetilde{\mathbf{Y}}}$, where $\sqrt{\cdot}$ is applied element-wise, due to the reduced noise level in $\sqrt{\widetilde{\mathbf{Y}}}$. Thus, we consider the magnitude measurement model (1).

In [23], the state-of-the-art SC-PRIME algorithm is devised for the conventional formulation (4) based on BSUM, which, however, does not take full advantage of modern parallel hardware architectures. Also, the conservative majorization in SC-PRIME often results in slow convergence. Therefore, we develop the *compact-SCAphase* and *SCAphase* algorithms for the compact formulation (3) and conventional formulation (4), respectively, based on an extension of SCA framework. Both proposed algorithms can be easily parallelized.

The two proposed algorithms are advantageous in different scenarios. The conventional formulation (4) is not suitable for large-scale problems due to the introduction of auxiliary variables. Also, the complexity of tuning two regularization parameters μ and ρ in (4) is significantly higher than that of tuning one parameter. However, compared to SCAphase, the computational complexity of compact-SCAphase grows dramatically with the increase of diversity of the designed linear measurement operator $\mathcal{F}$. Moreover, the conventional formulation (4) admits simple incorporation of additional prior information on $\mathbf{X}$ such as nonnegativity in radio astronomy [4].

In the following, we describe the proposed compact-SCAphase and SCAphase algorithms. The derivations are based on the model with complex-valued variables. However, the same derivations can be made for the real-valued case.

III. PROPOSED ALGORITHM FOR FORMULATION cPRDL

In this section, by extending the SCA framework in [29], [31], we propose an efficient iterative algorithm to find a stationary point of (3) via a sequence of approximate problems that can be solved in parallel. We denote, in this section, the objective function in (3) by $h(\mathbf{D},\mathbf{Z})$, which can be written as the sum of two parts, $h(\mathbf{D},\mathbf{Z})=f(\mathbf{D},\mathbf{Z})+g(\mathbf{Z})$, where

$$f(\mathbf{D},\mathbf{Z})=\tfrac{1}{2}\|\mathbf{Y}-|\mathcal{F}(\mathbf{DZ})|\|_{\text{F}}^2 \quad\text{and}\quad g(\mathbf{Z})=\lambda\|\mathbf{Z}\|_1. \quad (5)$$

The problem is challenging since g is non-smooth and, more notably, f is nonsmooth and nonconvex. To overcome this difficulty, in each iteration, we first majorize f by a smooth function, which naturally leads to a majorization for the overall objective function h. Then, the majorizing function is only minimized approximately. In particular, we obtain a descent direction of the majorizing function by minimize exactly its convex approximation. The variable can then be updated along this descent direction with a suitable step-size, which can be efficiently obtained by exact line search. Consequently, a decrease of the original objective function h is also ensured.

From the procedure described above, it can be noticed that the convergence of the proposed compact-SCAphase algorithm cannot be established under the framework of MM or SCA since the gradient consistency condition [32, A2.2] is apparently not satisfied. Nonetheless, in Section V-A, we prove that compact-SCAphase converges to a stationary point of problem (3) according to a generalized concept of stationarity.

Once a stationary point $(\mathbf{D}^\star,\mathbf{Z}^\star)$ of the cPRDL problem in (3) has been obtained by the compact-SCAphase algorithm, we optionally perform a debiasing step similar to that in [33] to further improve the estimation quality, which solves an instance of the cPRDL problem with $\lambda=0$ and a restriction that the entries z_{pi} having zero values in $\mathbf{Z}^\star$ are fixed at zero.

A. Smooth Majorization

We first derive a smooth majorizing function for f in (5) by following a similar approach as in [23]. Let $(\mathbf{D}^{(t)},\mathbf{Z}^{(t)})$ be the current point at iteration t. Function f can be expanded as $f(\mathbf{D},\mathbf{Z})=\tfrac{1}{2}(\|\mathbf{Y}\|_{\text{F}}^2+\|\mathcal{F}(\mathbf{DZ})\|_{\text{F}}^2)-\text{tr}(\mathbf{Y}^{\text{H}}|\mathcal{F}(\mathbf{DZ})|)$. We note that

$$|x|=|x\cdot e^{\text{j}\phi}|\geq\Re(x\cdot e^{\text{j}\phi})\ \text{for any}\ x\in\mathbb{C}\ \text{and}\ \phi\in[0,2\pi), \quad (6)$$

and that equality holds for $\phi=-\arg(x)$. Defining $\mathbf{Y}^{(t)}=\mathbf{Y}\odot e^{\text{jarg}(\mathcal{F}(\mathbf{D}^{(t)}\mathbf{Z}^{(t)}))}$, where $e^{(\cdot)}$ and $\arg(\cdot)$ are applied element-wise, we construct the following function:

$$\widehat{f}^{(t)}(\mathbf{D},\mathbf{Z})=-\text{tr}\Big(\mathbf{Y}^{\text{H}}\Re\big(\mathcal{F}(\mathbf{DZ})\odot e^{-\text{jarg}(\mathcal{F}(\mathbf{D}^{(t)}\mathbf{Z}^{(t)}))}\big)\Big)$$
$$+\tfrac{1}{2}(\|\mathbf{Y}\|_{\text{F}}^2+\|\mathcal{F}(\mathbf{DZ})\|_{\text{F}}^2)=\tfrac{1}{2}\|\mathbf{Y}^{(t)}-\mathcal{F}(\mathbf{DZ})\|_{\text{F}}^2. \quad (7)$$

As $\mathbf{Y}$ contains nonnegative entries, we can infer from (6) that $\widehat{f}^{(t)}(\mathbf{D},\mathbf{Z})\geq f(\mathbf{D},\mathbf{Z})$ for all $(\mathbf{D},\mathbf{Z})$, and $\widehat{f}^{(t)}(\mathbf{D}^{(t)},\mathbf{Z}^{(t)})=f(\mathbf{D}^{(t)},\mathbf{Z}^{(t)})$. Therefore, $\widehat{f}^{(t)}$ is a majorizing function of f at point $(\mathbf{D}^{(t)},\mathbf{Z}^{(t)})$ [32], [34] and, furthermore, function $\widehat{h}^{(t)}(\mathbf{D},\mathbf{Z})=\widehat{f}^{(t)}(\mathbf{D},\mathbf{Z})+g(\mathbf{Z})$ is a majorizing function of the objective function h at $(\mathbf{D}^{(t)},\mathbf{Z}^{(t)})$. The smooth majorizing function $\widehat{f}^{(t)}$ has the following partial gradients:

$$\nabla_{\mathbf{D}}\widehat{f}^{(t)}(\mathbf{D},\mathbf{Z})=\mathcal{F}^*\big(\mathcal{F}(\mathbf{DZ})-\mathbf{Y}^{(t)}\big)\cdot\mathbf{Z}^{\text{H}},$$
$$\nabla_{\mathbf{Z}}\widehat{f}^{(t)}(\mathbf{D},\mathbf{Z})=\mathbf{D}^{\text{H}}\cdot\mathcal{F}^*\big(\mathcal{F}(\mathbf{DZ})-\mathbf{Y}^{(t)}\big). \quad (8)$$

However, $\widehat{f}^{(t)}$ is nonconvex due to the bilinear map $\mathbf{DZ}$.

B. Separable Convex Approximation

Next, departing from the classic MM algorithm [32], [34], where $\widehat{h}^{(t)}$ is minimized exactly at a high computational cost,

we minimize $\widehat{h}^{(t)}$ inexactly via a convex approximation that can be decomposed into subproblems and solved in parallel.

Since the regularization g is convex and separable in all entries of $\mathbf{Z}$, we leave g unaltered and only design a separable convex approximate function for $\widehat{f}^{(t)}$. Although $\widehat{f}^{(t)}$ is not jointly convex, it is convex in each argument $\mathbf{D}$ and $\mathbf{Z}$, respectively. Hence, we adopt the best-response approximation, where the approximate function is the sum of several component functions [29]. In each component, only part of the variables are varied while the rest are fixed to their values at the current point $(\mathbf{D}^{(t)},\mathbf{Z}^{(t)})$. Let $\widetilde{f}_D^{(t)}(\mathbf{D})$ and $\widetilde{f}_Z^{(t)}(\mathbf{Z})$ be the approximate functions of $\widehat{f}^{(t)}$ over $\mathbf{D}$ and $\mathbf{Z}$, respectively. The best-response approximations are constructed as

$$\widetilde{f}_D^{(t)}(\mathbf{D})=\textstyle\sum_{p=1}^{P}\widehat{f}^{(t)}(\mathbf{d}_p,\mathbf{D}_{-p}^{(t)},\mathbf{Z}^{(t)}), \tag{9a}$$

$$\widetilde{f}_Z^{(t)}(\mathbf{Z})=\textstyle\sum_{i=1}^{I}\sum_{p=1}^{P}\widehat{f}^{(t)}(z_{pi},\mathbf{D}^{(t)},\mathbf{Z}_{-pi}^{(t)}), \tag{9b}$$

where $\mathbf{D}_{-p}$ is the $N\times(P-1)$ matrix obtained by removing column $\mathbf{d}_p$ from $\mathbf{D}$ and $\mathbf{Z}_{-pi}$ the collection of all entries of $\mathbf{Z}$ except z_{pi}. Then, the convex approximation of $\widehat{h}^{(t)}$ is $\widetilde{h}^{(t)}(\mathbf{D},\mathbf{Z})=\widetilde{f}_D^{(t)}(\mathbf{D})+\widetilde{f}_Z^{(t)}(\mathbf{Z})+\lambda\|\mathbf{Z}\|_1$ and the approximate problem at the t-th iteration reads

$$(\widetilde{\mathbf{D}}^{(t)},\widetilde{\mathbf{Z}}^{(t)})=\operatorname*{argmin}_{\mathbf{D}\in\mathcal{D},\mathbf{Z}}\widetilde{h}^{(t)}(\mathbf{D},\mathbf{Z}). \tag{10}$$

The columns of $\mathbf{D}$ and all the entries of $\mathbf{Z}$ are separable in the objective function of problem (10). Moreover, the constraint set $\mathcal{D}$ is a Cartesian product of compact convex sets, with each set corresponding to one column $\mathbf{d}_p$. Consequently, problem (10) can be decomposed into $P+(P\times I)$ subproblems. Each subproblem exclusively depends on a column $\mathbf{d}_p$ or a single variable z_{pi} and, hence, can be solved in parallel.

Define $\Delta\mathbf{D}=\widetilde{\mathbf{D}}^{(t)}-\mathbf{D}^{(t)}$ and $\Delta\mathbf{Z}=\widetilde{\mathbf{Z}}^{(t)}-\mathbf{Z}^{(t)}$. According to [29, Prop. 1], the difference $(\Delta\mathbf{D},\Delta\mathbf{Z})$ is a descent direction of the majorizing function $\widehat{h}^{(t)}$ in the domain of (3). Thus, the following simultaneous update rule can be applied:

$$\mathbf{D}^{(t+1)}=\mathbf{D}^{(t)}+\gamma^{(t)}\Delta\mathbf{D}\quad\text{and}\quad\mathbf{Z}^{(t+1)}=\mathbf{Z}^{(t)}+\gamma^{(t)}\Delta\mathbf{Z}, \tag{11}$$

where $\gamma^{(t)}\in[0,1]$ is the step-size. When $(\widetilde{\mathbf{D}}^{(t)},\widetilde{\mathbf{Z}}^{(t)})=(\mathbf{D}^{(t)},\mathbf{Z}^{(t)})$, a stationary point, in fact, a global minimizer, of $\widetilde{h}^{(t)}$ is achieved, which is also stationary for the majorizing problem and the original problem (3) (see Appendix C).

In the following, we describe the efficient solution approaches for the subproblems decomposed from (10).

Descent Direction for D. The P independent subproblems decomposed from problem (10) involving $\mathbf{D}$ can be written as

$$\min_{\mathbf{d}_p}\widehat{f}^{(t)}(\mathbf{d}_p,\mathbf{D}_{-p}^{(t)},\mathbf{Z}^{(t)})\qquad\text{s.t.}\quad\tfrac{1}{2}(\|\mathbf{d}_p\|_2^2-1)\leq0. \tag{12}$$

Each subproblem in (12) is an ℓ_2-norm constrained LS, which has no closed-form solution. However, as Slater's condition is satisfied for (12), strong duality holds and, hence, the primal and dual optimal solutions can be obtained by solving the Karush-Kuhn-Tucker (KKT) optimality system [35, 5.5.3]. By vectorization, we express $\widehat{f}^{(t)}(\mathbf{d}_p,\mathbf{D}_{-p}^{(t)},\mathbf{Z}^{(t)})$ as

$$\widehat{f}^{(t)}(\mathbf{d}_p,\mathbf{D}_{-p}^{(t)},\mathbf{Z}^{(t)})=\tfrac{1}{2}\|\operatorname{vec}(\mathbf{Y}_p^{(t)})-\mathbf{H}_p\mathbf{d}_p\|_2^2, \tag{13}$$

where $\mathbf{H}_p=\mathbf{F}(\mathbf{z}_{p:}^{(t)}\otimes\mathbf{I}_N)\in\mathbb{C}^{M_1M_2\times N}$ with $\mathbf{F}$ defined in (2), and $\mathbf{Y}_p^{(t)}=\mathbf{Y}^{(t)}-\mathcal{F}(\mathbf{D}_{-p}^{(t)}\mathbf{Z}_{-p}^{(t)})$ with $\mathbf{Z}_{-p}$ being the $(P-1)\times I$ matrix obtained by removing the p-th row of $\mathbf{Z}$. Then, the Lagrangian $L(\mathbf{d}_p,\nu_p)$ associated with problem (12) is

$$L(\mathbf{d}_p,\nu_p)=\tfrac{1}{2}\|\operatorname{vec}(\mathbf{Y}_p^{(t)})-\mathbf{H}_p\mathbf{d}_p\|_F^2+\tfrac{\nu_p}{2}(\|\mathbf{d}_p\|_2^2-1), \tag{14}$$

where $\nu_p\geq0$ is a Lagrangian multiplier. Let $\widetilde{\mathbf{d}}_p^{(t)}$ and $\widetilde{\nu}_p^{(t)}$ be any pair of primal and dual optimal solutions, and let $\mathbf{H}_p=\mathbf{U}\boldsymbol{\Sigma}\mathbf{V}^H$ be the compact singular value decomposition (SVD) of $\mathbf{H}_p$ and $\sigma_1\geq...\geq\sigma_r>0$ the nonzero singular values with $r=\operatorname{rank}(\mathbf{H}_p),\mathbf{U}\in\mathbb{C}^{M_1M_2\times r},\boldsymbol{\Sigma}\in\mathbb{C}^{r\times r}$, and $\mathbf{V}\in\mathbb{C}^{N\times r}$. Solving the KKT system, we can express the optimal solution $\widetilde{\mathbf{d}}_p^{(t)}$ of problem (12) as

$$\widetilde{\mathbf{d}}_p^{(t)}=\mathbf{V}\left(\boldsymbol{\Sigma}^H\boldsymbol{\Sigma}+\widetilde{\nu}_p^{(t)}\mathbf{I}_r\right)^{\dagger}\boldsymbol{\Sigma}^H\mathbf{U}^H\operatorname{vec}(\mathbf{Y}_p^{(t)}). \tag{15}$$

Defining the rational function ψ_p as

$$\psi_p(\nu_p)=\sum_{i=1}^{r}\frac{|c_{ip}|^2}{(\sigma_i^2+\nu_p)^2}, \tag{16}$$

where c_{ip} is the i-th entry of vector $\mathbf{c}_p$ defined as

$$\mathbf{c}_p=\boldsymbol{\Sigma}^H\mathbf{U}^H\operatorname{vec}(\mathbf{Y}_p^{(t)}), \tag{17}$$

the dual optimal point $\widetilde{\nu}_p^{(t)}$ required in (15) is determined by

$$\widetilde{\nu}_p^{(t)}\begin{cases}=0, & \text{if } \psi_p(0)\leq1,\\ \in\{\nu_p>0|\psi_p(\nu_p)=1\}, & \text{if } \psi_p(0)>1.\end{cases} \tag{18}$$

In the case where $\psi_p(0)>1$, $\widetilde{\nu}_p^{(t)}$ is the unique solution of

$$\psi_p(\nu_p)=1\quad\text{for}\quad\nu_p\in(0,+\infty), \tag{19}$$

which has no closed-form expression, except for the case where all singular values σ_i are identical. In the general case, to solve (19), we develop an efficient iterative algorithm based on successive rational approximation (cf. [36], [37]), which is outlined in Algorithm 2 and will be described in Section III-D. The intermediate derivations of the primal and dual solutions in (15)-(18) from the KKT system are included in Appendix A.

For the particular cases with the linear operator $\mathcal{F}$ in (51) that are investigated in the simulations, the SVD of $\mathbf{H}_p$ can be calculated analytically given the SVD of $\mathbf{A}$. Hence, the complexity is significantly reduced compared to the general case where an iterative algorithm, e.g., QR algorithm [38], is needed to obtain the SVD of $\mathbf{H}_p$ for every column $\mathbf{d}_p$ in each iteration. Then, the proposed SCA algorithm for the cPRDL problem in (3) is competitive with that for the PRDL problem in (4) in terms of complexity. Details on the simplified solution approach for $\mathcal{F}$ in (51) can also be found in Appendix A.

Descent Direction for Z. The independent subproblem decomposed from problem (10) involving each entry z_{pi} is

$$\widetilde{z}_{pi}^{(t)}=\operatorname*{argmin}_{z_{pi}}\quad\widehat{f}^{(t)}(z_{pi},\mathbf{D}^{(t)},\mathbf{Z}_{-pi}^{(t)})+\lambda|z_{pi}|. \tag{20}$$

Each subproblem above is a LASSO [39] in Lagrangian form with a single variable. Partition matrix $\mathbf{F}$ in (2) into I blocks as

$$\mathbf{F}=[\mathbf{F}_1,...,\mathbf{F}_I]\text{ with }\mathbf{F}_i\in\mathbb{C}^{M_1M_2\times N}\text{ for all }i=1,...,I. \tag{21}$$

Subproblem (20) admits a closed-form solution [39]

$$\widetilde{z}_{pi}^{(t)}=\frac{1}{\|\mathbf{F}_i\mathbf{d}_p^{(t)}\|_2^2}\mathcal{S}_\lambda\left(\|\mathbf{F}_i\mathbf{d}_p^{(t)}\|_2^2 z_{pi}^{(t)}-\nabla_{z_{pi}}\widehat{f}^{(t)}(\mathbf{D}^{(t)},\mathbf{Z}^{(t)})\right). \tag{22}$$

C. Step-size Computation

The majorizing function $\widehat{h}^{(t)}$ is nonsmooth due to the regularization g. Thus, to efficiently find a proper step-size $\gamma^{(t)}$ for the update in (11), we follow [29] and perform an exact line search on a differentiable upper bound of $\widehat{h}^{(t)}$. Ignoring constants, we can write the computation of step-size $\gamma^{(t)}$ as

$$\gamma^{(t)}=\operatorname*{argmin}_{0\leq\gamma\leq1}\left\{\begin{array}{l}\widehat{f}^{(t)}\left(\mathbf{D}^{(t)}+\gamma\Delta\mathbf{D},\mathbf{Z}^{(t)}+\gamma\Delta\mathbf{Z}\right)\\ +\gamma(g(\widetilde{\mathbf{Z}}^{(t)})-g(\mathbf{Z}^{(t)}))\end{array}\right\}, \tag{23}$$

Algorithm 1: compact-SCAphase

Input: $\mathbf{Y}\in\mathbb{R}_+^{M_1\times M_2}$, $\lambda\geq0$, $\varepsilon>0$.

1. Initialize $\mathbf{D}^{(0)}\in\mathcal{D}$ and $\mathbf{Z}^{(0)}$ randomly, $t\leftarrow0$;
2. **while** *stopping criterion (30) not achieved* **do**
3.   **for** $p=1,...,P$ **do** in parallel
4. $\mathbf{H}_p\leftarrow\mathbf{F}\cdot\big(\mathbf{z}_{p:}^{(t)}\otimes\mathbf{I}_N\big)$;
5.   Compute the SVD of $\mathbf{H}_p$: $\mathbf{H}_p=\mathbf{U}\mathbf{\Sigma}\mathbf{V}^{\mathrm{H}}$;
6.   Compute dual optimal value $\nu_p^{(t)}$ using (18);
7.   Compute $\widetilde{\mathbf{d}}_p^{(t)}$ according to (15);
8.   **for** $p=1,...,P, i=1,...,I$ **do** in parallel
9.   Compute $\widetilde{z}_{pi}^{(t)}$ according to (22);
10.   Compute step-size $\gamma^{(t)}$ by exact line search (23);
11.   Update the selected block variables using (11);
12. $t\leftarrow t+1$;
13. **return** $\mathbf{D}^{(t)},\mathbf{Z}^{(t)}$;

Algorithm 2: Rational approximation for solving (19)

Input: Rational function $\psi(\nu)$, tolerance $\eta>0$.

1. Initialize $\nu^{(0)}\leftarrow0, l\leftarrow0$;
2. **while** $\psi(\nu^{(l)})>1+\eta$ **do**
3. $\nu^{(l+1)}\leftarrow\nu^{(l)}+\frac{2\psi(\nu^{(l)})}{\psi'(\nu^{(l)})}\Big(1-\sqrt{\psi(\nu^{(l)})}\Big)$;
4. $l\leftarrow l+1$;
5. **return** $\nu^{(l)}$;

---

which corresponds to minimizing a fourth-order polynomial on the interval $[0,1]$ and can be solved by finding the real roots of its derivative, a third-order polynomial, in $[0,1]$. The analytical expressions of all three roots of a third-order polynomial in the complex domain are given by the well-known cubic formula. If there is more than one real root in $[0,1]$, evaluating the objective function in (23) is required to obtain $\gamma^{(t)}$.

Using the step-size $\gamma^{(t)}$ obtained by the line search (23) in the update (11), a monotonic decrease of the original objective function h in problem (3) is ensured, cf. [29]. We remark that the line search (23) always finds a nonzero step-size $\gamma^{(t)}$ since $(\Delta\mathbf{D},\Delta\mathbf{Z})$ is a descent direction of $\widehat{h}^{(t)}$, unless a stationary point of $\widehat{h}^{(t)}$ is attained, i.e., $(\Delta\mathbf{D},\Delta\mathbf{Z})$ are all-zero.

Finally, the proposed compact-SCAphase algorithm for solving the cPRDL problem in (3) is outlined in Algorithm 1.

D. Rational Approximation

Borrowing the idea in [36], [37], we develop a successive rational approximation algorithm, outlined in Algorithm 2, for efficiently solving the rational equation (19) in the general case, which corresponds to the dual optimal solution of subproblem (12). For simplicity, we omit the column index p in the derivations below where we discuss only one column.

Let $\nu^{(l)}$ be the approximate solution at iteration l. Function $\psi(\nu)$ decreases monotonically in $[0,+\infty)$ as all its poles are negative. Therefore, we interpolate function $\psi(\nu)$ around $\nu^{(l)}$ by a simple rational function

$$F(\nu;\alpha,\beta)=\frac{\alpha}{(\beta-\nu)^2}, \qquad (24)$$

where parameters α and β are chosen such that

$$F(\nu^{(l)};\alpha,\beta)=\psi(\nu^{(l)}), \quad F'(\nu^{(l)};\alpha,\beta)=\psi'(\nu^{(l)}).$$

Also, β represents the pole of F. It is easily verified that

$$\alpha=\frac{4\big(\psi(\nu^{(l)})\big)^3}{\big(\psi'(\nu^{(l)})\big)^2} \quad\text{and}\quad \beta=\nu^{(l)}+\frac{2\psi(\nu^{(l)})}{\psi'(\nu^{(l)})}. \qquad (25)$$

Then, the unique solution of $F(\nu;\alpha,\beta)=1$ in $(0,+\infty)$ is chosen as the next iterate $\nu^{(l+1)}$. Omitting intermediate calculations, we can express the update rule at the l-th iteration as

$$\nu^{(l+1)}=\nu^{(l)}+\frac{2\psi(\nu^{(l)})}{\psi'(\nu^{(l)})}\Big(1-\sqrt{\psi(\nu^{(l)})}\Big). \qquad (26)$$

Define $\delta_i=-\sigma_i^2$, for $i=1,...,r$, which are the poles of ψ with $\delta_1\leq...\leq\delta_r<0$. Ignoring the trivial case where all poles δ_i are identical, we derive the following bounding property.

Theorem 1: $F(\nu;\alpha,\beta)<\psi(\nu)$ for all $\nu>\delta_r$ and $\nu\neq\nu^{(l)}$.

Proof: See Appendix B.

Thus, if $\nu^{(l)}$ is below the solution $\widetilde{\nu}$ of the original rational function $\psi(\nu)=1$, i.e., $\psi(\nu^{(l)})>1$, then the solution of $F(\nu;\alpha,\beta)=1$ falls between $\nu^{(l)}$ and $\widetilde{\nu}$, i.e., $\nu^{(l)}<\nu^{(l+1)}<\widetilde{\nu}$. Hence, using the proposed rational approximation, we monotonically approach $\widetilde{\nu}$ from an initial point $\nu^{(0)}<\widetilde{\nu}$. Moreover, as we solve the rational equation in the case where $\psi(0)>1$, the dual variable ν can be simply initialized as $\nu^{(0)}=0$.

The theoretical convergence rate of Algorithm 2 can be shown to be of quadratic order, same as Newton's method. However, while Newton's method successively interpolates ψ by its tangent, Algorithm 2 instead interpolates ψ by a simple rational function, which leads to faster convergence due to the convexity of the rational functions in the considered interval. In the simulations, Algorithm 2 typically uses 3 or 4 iterations to achieve a precision of 10^{-9}.

E. Stopping Criterion

As mentioned in Section III-A, if $(\mathbf{D}^{(t)},\mathbf{Z}^{(t)})$ is stationary for the majorizing function $\widehat{h}^{(t)}$, it is also stationary for the original problem (3). Thus, to evaluate the quality of solution, we first derive the following stationarity condition for $\widehat{h}^{(t)}$ in the domain of problem (3) according to the relaxed C-stationarity defined in Section V-A: for all $p=1,...,P$, and $i=1,...,I$,

$$\nabla_{\mathbf{d}_p}\widehat{f}^{(t)}(\mathbf{D},\mathbf{Z})=\begin{cases}\mathbf{0}, & \|\mathbf{d}_p\|_2<1,\\ -\|\nabla_{\mathbf{d}_p}\widehat{f}^{(t)}(\mathbf{D},\mathbf{Z})\|_2\mathbf{d}_p, & \|\mathbf{d}_p\|_2=1,\end{cases} \qquad (27a)$$

and

$$\begin{cases}\nabla_{z_{pi}}\widehat{f}^{(t)}(\mathbf{D},\mathbf{Z})=-\lambda e^{\mathrm{jarg}(z_{pi})}, & z_{pi}\neq0,\\ |\nabla_{z_{pi}}\widehat{f}^{(t)}(\mathbf{D},\mathbf{Z})|\leq\lambda, & z_{pi}=0.\end{cases} \qquad (27b)$$

Then, we define the minimum-norm subgradient[1] $\nabla^S\widehat{h}^{(t)}$ of an extension of $\widehat{h}^{(t)}$ as follows [40]. At point $(\mathbf{D},\mathbf{Z})$, the component $\nabla^S_{\mathbf{d}_p}\widehat{h}^{(t)}(\mathbf{D},\mathbf{Z})$ of the minimum-norm subgradient with respect to column $\mathbf{d}_p$ is defined as

$$\begin{cases}\nabla_{\mathbf{d}_p}\widehat{f}^{(t)}(\mathbf{D},\mathbf{Z}), & \|\mathbf{d}_p\|_2<1,\\ \nabla_{\mathbf{d}_p}\widehat{f}^{(t)}(\mathbf{D},\mathbf{Z})+\|\nabla_{\mathbf{d}_p}\widehat{f}^{(t)}(\mathbf{D},\mathbf{Z})\|_2\mathbf{d}_p, & \|\mathbf{d}_p\|_2=1,\end{cases} \qquad (28)$$

---

[1]The name comes from the fact that it is the (Clarke) subgradient with the minimum Euclidean norm for the extended-value extension of $\widehat{h}^{(t)}$, where function values at points with $\mathbf{D}\notin\mathcal{D}$ are set to infinity.

and the component $\nabla^S_{z_{pi}}\widehat{h}^{(t)}(\mathbf{D},\mathbf{Z})$ of minimum-norm subgradient with respect to entry z_{pi} is defined as

$$\begin{cases} \nabla_{z_{pi}}\widehat{f}^{(t)}(\mathbf{D},\mathbf{Z})+\lambda e^{\mathrm{j}\arg(z_{pi})}, & z_{pi}\neq 0, \\ \max\{|\nabla_{z_{pi}}\widehat{f}^{(t)}(\mathbf{D},\mathbf{Z})|-\lambda,0\}, & z_{pi}=0. \end{cases} \quad (29)$$

The minimum-norm subgradient $\nabla^S\widehat{h}^{(t)}(\mathbf{D}^{(t)},\mathbf{Z}^{(t)})$ vanishes if and only if point $(\mathbf{D}^{(t)},\mathbf{Z}^{(t)})$ fulfills the stationarity conditions (27). This suggests that a reasonable termination criterion is that the minimum-norm subgradient must be small, i.e.,

$$\|\nabla^S_{\mathbf{D}}\widehat{h}^{(t)}(\mathbf{D}^{(t)},\mathbf{Z}^{(t)})\|_F\leq M_1 M_2\cdot\sqrt{NP}\cdot\varepsilon,$$
$$\text{and}\quad \|\nabla^S_{\mathbf{Z}}\widehat{h}^{(t)}(\mathbf{D}^{(t)},\mathbf{Z}^{(t)})\|_F\leq M_1 M_2\cdot\sqrt{PI}\cdot\varepsilon, \quad (30)$$

where $\varepsilon>0$ is a given tolerance, and the sizes of measurements and variables are also considered.

IV. PROPOSED ALGORITHM FOR FORMULATION PRDL

With the increase of diversity of designed linear measurement operator $\mathcal{F}$, the per-iteration complexity of compact-SCAphase dramatically grows due to the computation of partial Hessians and SVD of $\mathbf{H}_p$. Therefore, in this section, we propose the SCAphase algorithm for the conventional formulation (4) based on the same extended-SCA framework as in Section III.

Similarly, we denote the objective function in (4) by $h(\mathbf{X},\mathbf{D},\mathbf{Z})$ and decompose it into two parts: $h(\mathbf{X},\mathbf{D},\mathbf{Z})=f(\mathbf{X},\mathbf{D},\mathbf{Z})+g(\mathbf{Z})$, where $g(\mathbf{Z})=\rho\|\mathbf{Z}\|_1$ and

$$f(\mathbf{X},\mathbf{D},\mathbf{Z})=\tfrac{1}{2}\|\mathbf{Y}-|\mathcal{F}(\mathbf{X})|\|_F^2+\tfrac{\mu}{2}\|\mathbf{X}-\mathbf{D}\mathbf{Z}\|_F^2.$$

The first component f is nonconvex and nonsmooth, and the sparsity regularization g is convex but nonsmooth. In each iteration, we first find a descent direction by solving a separable convex approximate problem that is constructed based on a smooth majorizing function of f. Then, all variables are jointly updated along the descent direction by exact line search, which ensures a decrease of the original function h. An optional debiasing step, similar to that in Section III, can also be applied to the PRDL problem after a stationary point has been obtained, to further improve the estimation quality.

A. Smooth Majorization and Separable Convex Approximation

Let $(\mathbf{X}^{(t)},\mathbf{D}^{(t)},\mathbf{Z}^{(t)})$ be the current point at the t-th iteration, and define $\mathbf{Y}^{(t)}=\mathbf{Y}\odot e^{\mathrm{j}\arg(\mathcal{F}(\mathbf{X}^{(t)}))}$. Adopting the majorization technique (6), we first derive a smooth majorizing function $\widehat{f}^{(t)}$ for f at $(\mathbf{X}^{(t)},\mathbf{D}^{(t)},\mathbf{Z}^{(t)})$:

$$\widehat{f}^{(t)}(\mathbf{X},\mathbf{D},\mathbf{Z})=\tfrac{1}{2}\|\mathbf{Y}^{(t)}-\mathcal{F}(\mathbf{X})\|_F^2+\tfrac{\mu}{2}\|\mathbf{X}-\mathbf{D}\mathbf{Z}\|_F^2. \quad (31)$$

Thus, function $\widehat{h}^{(t)}(\mathbf{X},\mathbf{D},\mathbf{Z})=\widehat{f}^{(t)}(\mathbf{X},\mathbf{D},\mathbf{Z})+g(\mathbf{Z})$ is a majorizing function of the overall objective function h at $(\mathbf{X}^{(t)},\mathbf{D}^{(t)},\mathbf{Z}^{(t)})$. Function $\widehat{f}^{(t)}$ has the partial gradients

$$\nabla_{\mathbf{X}}\widehat{f}^{(t)}(\mathbf{X},\mathbf{D},\mathbf{Z})=\mathcal{F}^*(\mathcal{F}(\mathbf{X})-\mathbf{Y}^{(t)})+\mu(\mathbf{X}-\mathbf{D}\mathbf{Z}),$$
$$\nabla_{\mathbf{D}}\widehat{f}^{(t)}(\mathbf{X},\mathbf{D},\mathbf{Z})=\mu(\mathbf{D}\mathbf{Z}-\mathbf{X})\mathbf{Z}^{\mathrm{H}},$$
$$\nabla_{\mathbf{Z}}\widehat{f}^{(t)}(\mathbf{X},\mathbf{D},\mathbf{Z})=\mu\mathbf{D}^{\mathrm{H}}(\mathbf{D}\mathbf{Z}-\mathbf{X}). \quad (32)$$

We remark that $\widehat{f}^{(t)}$ is nonconvex due to the bilinear map $\mathbf{D}\mathbf{Z}$.

In the next step, we minimize a separable convex approximation of the majorizing function $\widehat{h}^{(t)}$, as $\widehat{h}^{(t)}$ is computationally expensive to minimize exactly. The best-response type approximate function of $\widehat{h}^{(t)}$ is designed as

$$\widetilde{h}^{(t)}(\mathbf{X},\mathbf{D},\mathbf{Z})=\widetilde{f}^{(t)}_X(\mathbf{X})+\widetilde{f}^{(t)}_D(\mathbf{D})+\widetilde{f}^{(t)}_Z(\mathbf{Z})+\rho\|\mathbf{Z}\|_1,$$

where $\widetilde{f}^{(t)}_X(\mathbf{X}),\widetilde{f}^{(t)}_D(\mathbf{D})$ and $\widetilde{f}^{(t)}_Z(\mathbf{Z})$ denote the approximate functions of $\widehat{f}^{(t)}$ over three block variables, respectively. The approximate functions $\widetilde{f}^{(t)}_D$ and $\widetilde{f}^{(t)}_Z$ are constructed in the same way as (9) in Section III. To limit the complexity of minimizing $\widetilde{h}^{(t)}$, we perform the best-response approximation on each entry of $\mathbf{X}$, which leads to the approximation

$$\widetilde{f}^{(t)}_X(\mathbf{X})=\sum_{i=1}^I\sum_{n=1}^N\widehat{f}^{(t)}(x_{ni},\mathbf{X}^{(t)}_{-ni},\mathbf{D}^{(t)},\mathbf{Z}^{(t)}),$$

where $\mathbf{X}_{-ni}$ is the collection of all entries of $\mathbf{X}$ except x_{ni}. The approximate problem at the t-th iteration then reads

$$(\widetilde{\mathbf{X}}^{(t)},\widetilde{\mathbf{D}}^{(t)},\widetilde{\mathbf{Z}}^{(t)})=\underset{\mathbf{X},\mathbf{D}\in\mathcal{D},\mathbf{Z}}{\arg\min}\widetilde{h}^{(t)}(\mathbf{X},\mathbf{D},\mathbf{Z}). \quad (33)$$

Likewise, problem (33) can be decomposed into $(N\times I)+P+(P\times I)$ independent subproblems. Each subproblem exclusively depends on a column $\mathbf{d}_p$ or a single variable x_{ni} or z_{pi} and, hence, can be solved in parallel.

Define $\Delta\mathbf{X}=\widetilde{\mathbf{X}}^{(t)}-\mathbf{D}^{(t)},\Delta\mathbf{D}=\widetilde{\mathbf{D}}^{(t)}-\mathbf{D}^{(t)}$, and $\Delta\mathbf{Z}=\widetilde{\mathbf{Z}}^{(t)}-\mathbf{Z}^{(t)}$. Then, the following simultaneous update rule along the descent direction $(\Delta\mathbf{X},\Delta\mathbf{D},\Delta\mathbf{Z})$ of $\widehat{h}^{(t)}$ is applied:

$$(\mathbf{X}^{(t+1)},\mathbf{D}^{(t+1)},\mathbf{Z}^{(t+1)})=(\mathbf{X}^{(t)},\mathbf{D}^{(t)},\mathbf{Z}^{(t)})+\gamma^{(t)}(\Delta\mathbf{X},\Delta\mathbf{D},\Delta\mathbf{Z}) \quad (34)$$

with $\gamma^{(t)}\in[0,1]$ being the step-size. When $(\widetilde{\mathbf{X}}^{(t)},\widetilde{\mathbf{D}}^{(t)},\widetilde{\mathbf{Z}}^{(t)})=(\mathbf{X}^{(t)},\mathbf{D}^{(t)},\mathbf{Z}^{(t)})$, the algorithm has converged to a stationary point of the convex approximation $\widetilde{h}^{(t)}$, which is also stationary for the majorization and the original problem (3).

In the following, the closed-form solutions for the subproblems decomposed from (33) are derived. First, the $N\times I$ independent subproblems involving $\mathbf{X}$ can be written as

$$\widetilde{x}^{(t)}_{ni}=\underset{x_{ni}}{\arg\min}\quad\widehat{f}^{(t)}(x_{ni},\mathbf{X}^{(t)}_{-ni},\mathbf{D}^{(t)},\mathbf{Z}^{(t)}). \quad (35)$$

Function $\widehat{f}^{(t)}$ is a quadratic function with respect to $\mathbf{X}$ and the ni-th diagonal entry of the Hessian is $\nabla^2_{x_{ni}}\widehat{f}^{(t)}=\|\mathbf{f}_{ni}\|_2^2+\mu$, where $\mathbf{f}_{ni}$ is the ni-th column of $\mathbf{F}$. Then, each subproblem (35) is a univariate quadratic program and has a solution

$$\widetilde{x}^{(t)}_{ni}=x^{(t)}_{ni}-\nabla_{x_{ni}}\widehat{f}^{(t)}(\mathbf{X}^{(t)},\mathbf{D}^{(t)},\mathbf{Z}^{(t)})/\nabla^2_{x_{ni}}\widehat{f}^{(t)}. \quad (36)$$

Next, the P independent subproblems decomposed from (33) that involve matrix $\mathbf{D}$ can be written as

$$\widetilde{\mathbf{d}}^{(t)}_p=\underset{\mathbf{d}_p}{\arg\min}\tfrac{1}{2}\|\mathbf{X}^{(t)}-\mathbf{D}^{(t)}_{-p}\mathbf{Z}^{(t)}_{-p}-\mathbf{d}_p(\mathbf{z}^{(t)}_{p:})^{\mathrm{T}}\|_F^2\quad\text{s.t.}\|\mathbf{d}_p\|_2\leq 1, \quad (37)$$

which can again be solved via the KKT optimality system. Unlike (12), problem (37) has a simple closed-form solution

$$\widetilde{\mathbf{d}}^{(t)}_p=\widehat{\mathbf{d}}_p/\max\{\|\widehat{\mathbf{d}}_p\|_2,1\}, \quad (38)$$

with $\widehat{\mathbf{d}}_p=\mathbf{d}^{(t)}_p-\nabla_{\mathbf{d}_p}\widehat{f}^{(t)}(\mathbf{X}^{(t)},\mathbf{D}^{(t)},\mathbf{Z}^{(t)})/(\mu\|\mathbf{z}^{(t)}_{p:}\|_2^2)$. Finally, each subproblem involving an entry z_{pi} is a Lagrangian form of univariate LASSO and has a closed-form solution [41]

$$\widetilde{z}^{(t)}_{pi}=\tfrac{1}{\|\mathbf{d}^{(t)}_p\|_2^2}\mathcal{S}_{\frac{\rho}{\mu}}\left(\|\mathbf{d}^{(t)}_p\|_2^2 z^{(t)}_{pi}-\tfrac{1}{\mu}\nabla_{z_{pi}}\widehat{f}^{(t)}(\mathbf{X}^{(t)},\mathbf{D}^{(t)},\mathbf{Z}^{(t)})\right). \quad (39)$$

B. Step-size Computation

Similarly to Section III-C, to efficiently find a step-size $\gamma^{(t)}$ for the update in (34) that ensures a decrease of the original function in (4), we perform an exact line search on a differentiable upper bound of $\widehat{h}^{(t)}$, which is formulated as

$$\gamma^{(t)}=\underset{0\leq\gamma\leq 1}{\arg\min}\left\{\begin{array}{l}\widehat{f}^{(t)}(\mathbf{X}^{(t)}+\gamma\Delta\mathbf{X},\mathbf{D}^{(t)}+\gamma\Delta\mathbf{D},\mathbf{Z}^{(t)}+\gamma\Delta\mathbf{Z})\\ +\gamma\big(g(\widetilde{\mathbf{Z}}^{(t)})-g(\mathbf{Z}^{(t)})\big)\end{array}\right\}, \quad (40)$$

Algorithm 3: SCAphase

Input: $\mathbf{Y} \in \mathbb{R}_+^{M_1 \times M_2}$, $\mu, \lambda \geq 0$, $\varepsilon > 0$.

1   Initialize $\mathbf{X}^{(0)}$ and $\mathbf{D}^{(0)} \in \mathcal{D}$ randomly,
     $\mathbf{Z}^{(0)} \leftarrow (\mathbf{D}^{(0)})^\dagger \mathbf{X}^{(0)}$, $t \leftarrow 0$;

2   **while** *stopping criterion* (43) *not achieved* **do**

3   **for** $n = 1,...,N, i = 1,...,I$ **do** in parallel

4   Compute $\widetilde{x}_{ni}^{(t)}$ according to (36);

5   **for** $p = 1,...,P$ **do** in parallel

6   Compute $\widetilde{\mathbf{d}}_p^{(t)}$ according to (38);

7   **for** $p = 1,...,P, i = 1,...,I$ **do** in parallel

8   Compute $\widetilde{z}_{pi}^{(t)}$ according to (39);

9   Compute step-size $\gamma^{(t)}$ by exact line search (40);

10   Update the selected block variables using (34);

11    $t \leftarrow t+1$;

12   **return** $\mathbf{X}^{(t)}, \mathbf{D}^{(t)}, \mathbf{Z}^{(t)}$;

---

which is also a minimization of fourth-order polynomial. Similarly, (40) can be solved analytically by rooting the derivative of the objective function; we omit the straightforward details.

Finally, the proposed SCAphase algorithm for solving the PRDL problem in (4) is outlined in Algorithm 3.

C. Stopping Criterion

If $(\mathbf{X}^{(t)}, \mathbf{D}^{(t)}, \mathbf{Z}^{(t)})$ is stationary for the majorizing function $\widehat{h}^{(t)}$, then it is also stationary for the original problem (4). Therefore, analogously to Section III-E, we first derive the stationarity condition for $\widehat{h}^{(t)}$ according to the concept of relaxed C-stationarity in Section V-A. Based on the stationarity condition, the minimum-norm subgradient of the extension of $\widehat{h}^{(t)}$ is introduced to evaluate the quality of the current solution.

Similar to (27), for a stationary point of $\widehat{h}^{(t)}$, the gradients $\nabla_\mathbf{D} \widehat{f}^{(t)}$ and $\nabla_\mathbf{Z} \widehat{f}^{(t)}$ given in (32) must satisfy the following conditions: for all $p = 1,...,P$, and $i = 1,...,I$,

$$\nabla_{\mathbf{d}_p} \widehat{f}^{(t)}(\mathbf{X}, \mathbf{D}, \mathbf{Z}) = \begin{cases} \mathbf{0}, & \|\mathbf{d}_p\|_2 < 1, \\ -\|\nabla_{\mathbf{d}_p} \widehat{f}^{(t)}(\mathbf{X}, \mathbf{D}, \mathbf{Z})\|_2 \mathbf{d}_p, & \|\mathbf{d}_p\|_2 = 1, \end{cases} \tag{41a}$$

and

$$\begin{cases} \nabla_{z_{pi}} \widehat{f}^{(t)}(\mathbf{X}, \mathbf{D}, \mathbf{Z}) = -\rho e^{j\arg(z_{pi})}, & z_{pi} \neq 0, \\ |\nabla_{z_{pi}} \widehat{f}^{(t)}(\mathbf{X}, \mathbf{D}, \mathbf{Z})| \leq \rho, & z_{pi} = 0. \end{cases} \tag{41b}$$

Then, the components of the minimum-norm subgradient with respect to matrices $\mathbf{Z}$ and $\mathbf{D}$ are defined in the same way as in Section III-E. As for the gradient with respect to matrix $\mathbf{X}$, stationarity simply requires the gradient $\nabla_\mathbf{X} \widehat{f}^{(t)}$ to vanish:

$$\nabla_\mathbf{X} \widehat{f}^{(t)}(\mathbf{X}, \mathbf{D}, \mathbf{Z}) = \mathbf{0}. \tag{42}$$

Thus, the component $\nabla_\mathbf{X}^S \widehat{h}^{(t)}$ of the minimum-norm subgradient with respect to $\mathbf{X}$ is simply defined as the gradient $\nabla_\mathbf{X} \widehat{f}^{(t)}$.

In summary, the stationary conditions of the majorizing function $\widehat{h}^{(t)}$ consist of the conditions (41)-(42). The algorithm is terminated when the minimum-norm subgradient at $(\mathbf{X}^{(t)}, \mathbf{D}^{(t)}, \mathbf{Z}^{(t)})$ is small, i.e., with a given tolerance $\varepsilon > 0$,

$$\begin{cases} \|\nabla_\mathbf{D}^S \widehat{h}^{(t)}(\mathbf{X}^{(t)}, \mathbf{D}^{(t)}, \mathbf{Z}^{(t)})\|_\mathrm{F} \leq M_1 M_2 \cdot \sqrt{NP} \cdot \varepsilon, \\ \|\nabla_\mathbf{Z}^S \widehat{h}^{(t)}(\mathbf{X}^{(t)}, \mathbf{D}^{(t)}, \mathbf{Z}^{(t)})\|_\mathrm{F} \leq M_1 M_2 \cdot \sqrt{PI} \cdot \varepsilon, \\ \|\nabla_\mathbf{X}^S \widehat{h}^{(t)}(\mathbf{X}^{(t)}, \mathbf{D}^{(t)}, \mathbf{Z}^{(t)})\|_\mathrm{F} \leq M_1 M_2 \cdot \sqrt{NI} \cdot \varepsilon. \end{cases} \tag{43}$$

D. Comparison with SC-PRIME

The proposed SCAphase algorithm and the state-of-the-art SC-PRIME [23] adopt the same formulation, i.e., the PRDL problem in (4), and the same successive majorization technique (31). However, there are two important differences between the two algorithms. First, SC-PRIME updates the variables in a block coordinate descent (BCD) manner, i.e., minimizes the majorizing function $\widehat{h}^{(t)}$ alternatively with respect to each block variable $\mathbf{X}$, $\mathbf{Z}$, and each column of $\mathbf{D}$, instead of using parallel updates. Then, to avoid the expensive exact minimization of $\widehat{h}^{(t)}$, SC-PRIME minimizes a different separable convex approximation for each block variable from SCAphase. Instead of using the best-response approximation, SC-PRIME further majorizes the LS function $\widehat{f}^{(t)}$ by replacing the partial Hessian with respect to a block variable by the identity matrix scaled by an upper bound of its eigenvalues. The minimizer of this majorization has a closed-form expression and gives a guaranteed decrease of the original objective function h without a step-size search. However, since the Hessian is typically ill-conditioned, this majorization tends to be conservative, which may lead to slow convergence. In contrast, the best-response approximation $\widetilde{f}^{(t)}$ equivalently preserves all diagonal entries of the Hessian but is not necessarily a majorization of the original function f. Thus, discarding the global upper bound constraint provides more flexibility in designing an approximation that yields faster convergence to a good stationary point. This advantage is demonstrated numerically in Section VI.

V. CONVERGENCE AND COMPLEXITY

A. Convergence Analysis

For a nonsmooth optimization, the gradient consistency condition [32, A2.2] in the classic MM algorithms and BSUM requires the consistency of directional derivatives between the original nonsmooth function and its majorant at the current point in all directions, which apparently cannot be satisfied at a non-differentiable point of the original function if the majorizing function is restricted to be smooth, such as in the proposed algorithms. On the other hand, the convergence in the SCA framework is only established for composite problems with smooth loss functions. Therefore, neither the convergence analysis of the MM algorithms nor that of the SCA framework can be directly applied to the proposed algorithms. Then, in this subsection, we establish the convergence of our proposed algorithms according to a generalized concept of stationarity.

To this end, we first introduce several generalizations of the subdifferential of a function, since the usual convex subdifferential does not exist at every point for a nonconvex function. Consider a general nonconvex nonsmooth function $f(\mathbf{s}) : \mathbb{R}^n \rightarrow \mathbb{R}$ that is locally Lipschitz [42, Def. 1], which basically implies that every neighborhood of a non-differentiable point of f contains a differentiable point. Thus, the Bouligand subdifferential $\partial_B f(\mathbf{s})$ of f exists at every point $\mathbf{s} \in \mathbb{R}^n$ and is defined as [42]

$$\partial_B f(\mathbf{s}) = \{\mathbf{r} \in \mathbb{R}^n | \exists \mathbf{s}^k \rightarrow \mathbf{s}, \nabla f(\mathbf{s}^k) \text{ exists}, \nabla f(\mathbf{s}^k) \rightarrow \mathbf{r}\}. \tag{44}$$

TABLE I: Computational complexity of dominant operations in each iteration

	computation of gradient	computation of partial Hessians	computation of polynomial coefficients in line search function
compact-SCAphase	$c(\mathcal{F})+4NPI$	general case: $4M_1M_2NPI+\mathcal{O}(M_1M_2N^2P)$; special case with $\mathcal{F}$ in (51): $2M_1NP+2M_2PI$	$2c(\mathcal{F})+6NPI$
SCAphase	$c(\mathcal{F})+4NPI$	$2NP+2PI$	$c(\mathcal{F})+6NPI$
SC-PRIME	$2c(\mathcal{F})+6NPI$	–	–

The Clarke subdifferential (C-subdifferential) of f at $\mathbf{s}$ is then defined as the convex hull of $\partial_B f(\mathbf{s})$ [42]:

$$\partial_C f(\mathbf{s})=\mathrm{conv}(\partial_B f(\mathbf{s})). \tag{45}$$

To further generalize the concept of stationarity to non-Lipschitz functions, in [43], the author introduced a new definition of C-subdifferential for any function, which is consistent with the previous definition in (45) for the Lipschitz case. The extended definition of C-subdifferential is omitted since it is not required in the proof of convergence in this paper.

Now consider a general constrained problem

$$\min_{\mathbf{s}\in\mathcal{C}} f(\mathbf{s}), \tag{46}$$

where f is locally Lipschitz and $\mathcal{C}\subseteq\mathbb{R}^n$ is a closed convex set. One possible generalization of stationarity for the constrained nonsmooth problem (46) is the Clarke stationarity (C-stationarity) [42], which, however, is not easy to verify. Hence, we introduce the following relaxed C-stationarity.

Definition 2: (Relaxed C-stationarity). A point $\mathbf{s}\in\mathbb{R}^n$ is said to be a relaxed C-stationary point of problem (46) if it satisfies

$$\mathbf{0}\in\partial_C f(\mathbf{s})+\partial_C\mathbb{I}_{\mathcal{C}}(\mathbf{s}), \tag{47}$$

where $\mathbb{I}_{\mathcal{C}}$ is the indicator function of set $\mathcal{C}$ and defined as

$$\mathbb{I}_{\mathcal{C}}(\mathbf{s})=\begin{cases} 0, & \text{if } \mathbf{s}\in\mathcal{C}, \\ +\infty, & \text{otherwise}, \end{cases} \tag{48}$$

and $\partial_C\mathbb{I}_{\mathcal{C}}(\mathbf{s})$ is equal to the normal cone of $\mathcal{C}$ at $\mathbf{s}$ by the extended definition in [43, Def. 2.4.10], as $\mathbb{I}_{\mathcal{C}}$ is non-Lipschitz.

Definition 2 is motivated by the following two facts. First, condition (47) is a necessary condition for $\mathbf{s}$ being a local minimal point of problem (46) [43, Prop. 2.4.3], but not sufficient unless problem (46) is convex, which is similar to the usual stationarity condition in the smooth case. Second, Definition 2 is consistent with the usual concept of stationarity in the special cases where the problem is smooth or convex. Particularly, the stationarity conditions in (27) and (41) for the majorization in compact-SCAphase and SCAphase, respectively, are special cases of condition (47). Additionally, as the name suggests, the set of C-stationary points is a subset of relaxed C-stationary points, which can be shown by the sum rule of C-subdifferential [43, Prop. 2.3.3]. Although the above definitions of subdifferentials and stationarity are described for a problem with real-valued variables, the same concepts can be immediately extended to the complexed-valued case.

Then, with the generalized concept of stationarity, we claim that the solution sequence of the compact-SCAphase algorithm converges according to the following proposition.

Theorem 3: Every limit point of the solution sequence $\{\mathbf{D}^{(t)},\mathbf{Z}^{(t)}\}_t$ generated by the compact-SCAphase algorithm is a relaxed C-stationary point of problem (3).

Proof: See Appendix C.

A similar theorem can be claimed for the SCAphase algorithm, since compact-SCAphase and SCAphase can be viewed as instantiations of the same extended SCA framework on different problem formulations.

The classic MM algorithms possess the convergence to the set of directional stationary points [32], which is shown to be a subset of C-stationary points in [42] and, hence, is also a subset of relaxed C-stationary points. Therefore, compared to the classic MM algorithms, which can only be used in our problem with a nonsmooth upper bound and high computational complexity, in the proposed algorithms, we basically sacrifice the strictness of the stationarity in order to construct a surrogate problem that can be easily addressed.

In [23], the authors address the convergence of SC-PRIME, which employs the same smooth majorization in (6), under the framework of BSUM [44]. However, the convergence analysis in [23] is incomplete since the authors ignored the aforementioned fact that the gradient consistency condition required by BSUM cannot be satisfied at non-differentiable points of the original function. The convergence analysis in Appendix C can be used to fill this gap and justify that the SC-PRIME algorithm converges to a stationary point of problem (4) corresponding to the same generalized concept of stationarity, i.e., relaxed C-stationarity.

In addition, another extension of SCA framework is proposed in [45] based on the difference of convex technique, which differs from our proposed algorithm in the following two aspects. First, the algorithm in [45] tackles a composite problem with a smooth but not necessarily convex loss function and a nonconvex nonsmooth regularization, whereas in this paper, as shown in (3) and (4), a composite problem with a nonconvex nonsmooth loss function and a convex but not necessarily smooth regularization is addressed. Second, a different generalization of stationarity is employed in [45] to establish the convergence. The set of relaxed C-stationary points can be shown to be a subset of the stationary points defined in [45], similarly, by the sum rule of C-subdifferential.

B. Computational Complexity

In this subsection, we present a theoretic comparison on the complexity of the proposed algorithms, compact-SCAphase and SCAphase, and the state-of-the-art SC-PRIME [23].

As presented in Table I, for each algorithm, we count the total number of flops [38] required by the dominant operations, such as matrix-matrix multiplication, in each iteration, which reflects the per-iteration complexity in the worst case where the flops are executed in sequence. The per-iteration complexity of the proposed algorithms are mainly dominated by three components: the computation of gradient and partial Hessians
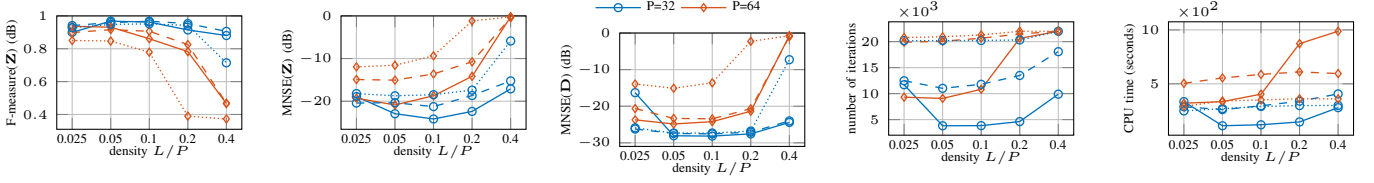
Fig. 1: Multi-antenna Random Access Network

of the smooth majorization $\widehat{f}^{(t)}$, which are required for solving the convex subproblems, and the computation of polynomial coefficients of the line search function in the step-size computation. In the simulations, the rational approximation algorithm employed by compact-SCAphase for solving the subproblems requires 3 or 4 iterations to achieve a precision of 10^{-9}. Therefore, the complexity of the rational approximation is comparable to that of computing a closed-form solution as in SCAphase and SC-PRIME, which is negligible compared to the other operations. In Table I, $c(\mathcal{F})$ stands for the complexity of the linear operator $\mathcal{F}$ or, equivalently, that of its adjoint $\mathcal{F}^*$, which depends on the structure of $\mathcal{F}$ and the specific implementation. In principle, $c(\mathcal{F})$ admits the bounds $2NI \cdot \max\{M_1, M_2\} \leq c(\mathcal{F}) \leq 2M_1 M_2 NI$.

Compared to SCAphase, in the general case, compact-SCAphase has a per-iteration complexity of higher order due to the computation of partial Hessians and SVD of matrix $\mathbf{H}_p$ in (13). However, in the special case with the linear operator $\mathcal{F}$ in (51), such as Cases 1 and 2 in the simulations, the complexity of computation of partial Hessians in compact-SCAphase dramatically decreases and the SVD of $\mathbf{H}_p$ can be analytically calculated given the SVD of $\mathbf{A}$. Then, compact-SCAphase and SCAphase have comparable per-iteration complexity. On the other hand, as shown in Fig. 2, compared to SCAphase, compact-SCAphase typically uses half the number of iterations to achieve a stationary point due to the reduction of variables, which makes compact-SCAphase more competitive than SCAphase in the case with $\mathcal{F}$ in (51).

Next, we compare the complexity of SCAphase and SC-PRIME. The line search is not required in SC-PRIME as it employs the BCD update. In the specific implementation of SC-PRIME used in this paper, some constant rough upper bounds for the eigenvalues of the partial Hessians are used to construct the surrogate subproblems and, hence, only the gradient of $\widehat{f}^t$ is needed. However, compared to SC-PRIME, the additional line search in SCAphase does not cause a significant increase on the overall per-iteration complexity because several intermediate variables required in the computation of gradient can be updated recursively. For example, $\mathcal{F}(\mathbf{X}^{(t)})$ required in (32) is updated recursively by $\mathcal{F}(\mathbf{X}^{(t+1)})=\mathcal{F}(\mathbf{X}^{(t)})+\gamma^{(t)}\mathcal{F}(\Delta\mathbf{X})$, where $\mathcal{F}(\Delta\mathbf{X})$ is already calculated in the computation of coefficients of line search function. Thus, SCAphase and SC-PRIME also have similar per-iteration complexity, especially in the case with a highly diverse linear operator $\mathcal{F}$, where the per-iteration complexity is dominated by the complexity of $\mathcal{F}$. On the other hand, with the additional line search, SCAphase exhibits faster convergence in terms of number of iterations.

Finally, we remark that, in contrast to the BCD update in SC-PRIME, the computation of solutions of subproblems in compact-SCAphase and SCAphase can be fully parallelized with suitable hardware architectures.

VI. SIMULATION RESULTS

In this section, we compare the performance of the two proposed algorithms and the state-of-the-art SC-PRIME [23] on synthetic data in the context of blind channel estimation in a multi-antenna random access network. All experiments were conducted on a Linux machine assigned with two 2.3 GHz cores and 7 GB RAM running MATLAB R2021b. Although, theoretically, all the subproblems in each iteration in the proposed algorithms can be solved in parallel, for simplicity, the subproblems involving different block variables (i.e., $\mathbf{X}$, $\mathbf{D}$, or $\mathbf{Z}$) are solved sequentially, whereas the computation of solutions for subproblems involving the same block variable are parallelized by using vectorization in MATLAB.

A. Simulation Setup

We consider a multi-antenna random access network with magnitude-only measurements as depicted in Fig. 1. The base station is equipped with N antennas and P single-antenna users with unknown spatial signatures $\{\mathbf{d}_p \in \mathbb{C}^N\}_{p=1}^P$ sporadically access the channel in I time-slots. In time-slot i user p transmits an unknown information symbol $z_{pi} \neq 0$ with probability L/P and $z_{pi}=0$ with probability $(P-L)/P$, where L defines the expected sparsity level of the transmitted symbol vectors $\mathbf{z}_i=[z_{1i},...,z_{Pi}]^{\mathrm{T}}, i=1,...,I$. Then, with $\mathbf{D}=[\mathbf{d}_1,...,\mathbf{d}_P]$, the received symbol vector $\mathbf{x}_i=[x_{1i},...,x_{Ni}]^{\mathrm{T}}$ at the antennas is given by $\mathbf{x}_i=\mathbf{D}\mathbf{z}_i$, which cannot be observed directly. The objective is to jointly learn the spatial signature matrix $\mathbf{D}$ and the sparse transmitted symbol vectors $\mathbf{z}_i$ from spatially and temporally filtered subband magnitude measurements that can be acquired at a reduced sampling rate. More precisely, the antenna signals $\mathbf{X}$ undergo a linear transformation

$$\mathcal{F}(\mathbf{X})=\sum_{k=1}^K \mathbf{A}_k \mathbf{X} \mathbf{B}_k, \tag{49}$$

which, as shown in Fig. 1, can be interpreted as K independent chains of designed linear spatial mixing networks $\{\mathbf{A}_k \in \mathbb{C}^{M_1 \times N}\}_{k=1}^K$ and temporal mixing networks $\{\mathbf{B}_k \in \mathbb{C}^{I \times M_2}\}_{k=1}^K$. We remark that the order of the spatial mixing $\mathbf{A}_k$ and temporal mixing $\mathbf{B}_k$ are interchangeable for each chain. Matrix $\mathbf{F}$ in the vectorized form (2) corresponding to $\mathcal{F}$ in (49) is

$$\mathbf{F}=\sum_{k=1}^K \mathbf{B}_k^{\mathrm{T}} \otimes \mathbf{A}_k. \tag{50}$$

In our simulations, the spatial mixing networks $\{\mathbf{A}_k\}_{k=1}^K$ are generated from a complex Gaussian distribution, and the following three particular cases of linear operator $\mathcal{F}$ of different levels of diversity are investigated:

- *Case 1: Time-invariant spatial mixing and no temporal mixing.* In this case, $\mathcal{F}$ is interpreted by a single chain of mixing networks, i.e., $K=1$. For simplicity, we omit the subscript on the mixing networks and $\mathcal{F}$ reduces to

$$\mathcal{F}(\mathbf{X})=\mathbf{A}\mathbf{X}\mathbf{B}. \tag{51}$$

Moreover, the temporal mixing is set to be $\mathbf{B}=\mathbf{I}$.

Fig. 2: Performance vs. density L/P using compact-SCAphase (solid), SCAphase (dashed), and SC-PRIME (dotted) in Case 1. $N=64, M_1=4N, I=16N$.

- *Case 2: Time-invariant spatial mixing and STFT temporal mixing.* In this case, $\mathcal{F}$ can also be expressed by the model (51), whereas the temporal mixing $\mathbf{B}$ is designed to be the short-time Fourier transform (STFT) [16], which can be implemented by analog subband filters.
- *Case 3: Time-variant spatial mixing and no temporal mixing.* In this case, $\mathcal{F}$ is expressed by the model (49) with $K=I$, and the k-th temporal mixing is set to be $\mathbf{B}_k=[\mathbf{0},...,\mathbf{0},\mathbf{e}_k,\mathbf{0},...,\mathbf{0}]$ with $\mathbf{e}_k$ being a standard basis vector, which simply selects the k-th snapshot. Also, $\mathbf{A}_k$ is the spatial mixing network designed for the k-th snapshot.

The basic simulation setup is as follows. In each time-slot i, L randomly selected elements of the true transmitted sparse signal $\mathbf{z}_i^{\text{true}}$ are set to be nonzero. The nonzero elements of matrix $\mathbf{Z}^{\text{true}}$, all elements of spatial mixing matrices $\{\mathbf{A}_k\}_{k=1}^K$ and the true spatial signature $\mathbf{D}^{\text{true}}$ are drawn from an i.i.d. standard complex Gaussian distribution. The magnitude measurements $\mathbf{Y}$ are generated according to (1) with additive white Gaussian noise. The number of Monte-Carlo runs is 50.

From the solutions $\mathbf{D}$ and $\mathbf{Z}$ obtained by compact-SCAphase, the variable $\mathbf{X}$ is constructed as $\mathbf{X}=\mathbf{DZ}$ for the performance evaluation. In some other applications, such as diffraction imaging, the signal $\mathbf{X}$ is the main target for estimation, whereas the dictionary $\mathbf{D}$ and sparse code matrix $\mathbf{Z}$ are merely artifacts used to improve the estimation of $\mathbf{X}$. In contrast, as shown in Fig. 1, our main target is the spatial signature matrix $\mathbf{D}$ and transmitted signals $\mathbf{Z}$. Hence, only the estimation qualities of $\mathbf{D}$ and $\mathbf{Z}$ are presented in the following simulations. However, the solution $\mathbf{X}$ is still required in the disambiguation step, which is described afterwards.

Note that, in both formulations (3) and (4), the variables $\mathbf{X}, \mathbf{D}$, and $\mathbf{Z}$ can only be recovered up to three trivial ambiguities if no additional constraint on $\mathbf{X}$ is given. Specifically, any combination of the following three trivial operations conserve the magnitude measurements and the sparsity pattern of $\mathbf{Z}$: 1) Global phase shift: $(\mathbf{X},\mathbf{Z})\rightarrow(\mathbf{X}e^{\mathrm{j}\phi},\mathbf{Z}e^{\mathrm{j}\phi})$, 2) Scaling: $(\mathbf{d}_p,\mathbf{z}_{p:})\rightarrow(\alpha_p\mathbf{d}_p,\alpha_p^{-1}\mathbf{z}_{p:})$ with any $\alpha_p\in\mathbb{C}$ and $\alpha_p\neq0$, 3) Permutation: $(\mathbf{D},\mathbf{Z})\rightarrow(\mathbf{DP}^{\mathrm{T}},\mathbf{PZ})$ with any permutation matrix $\mathbf{P}\in\mathbb{R}^{P\times P}$. Also, in the case without temporal mixing, the global phase ambiguity holds column-wise, i.e., $(\mathbf{x}_i,\mathbf{z}_i)\rightarrow(\mathbf{x}_ie^{\mathrm{j}\phi_i},\mathbf{z}_ie^{\mathrm{j}\phi_i})$.

A disambiguation step is required to measure the estimation quality of the solutions. Let $\mathbf{X}^{\text{true}}=\mathbf{D}^{\text{true}}\mathbf{Z}^{\text{true}}$ be the true received signals. To resolve the global phase ambiguity, the solution $\mathbf{X}$ is corrected by the global phase shift $\phi^\star=\arg\min_{\phi\in[0,2\pi)}\|\mathbf{X}e^{\mathrm{j}\phi}-\mathbf{X}^{\text{true}}\|_{\mathrm{F}}^2$ in the case with temporal mixing, and the phase correction is applied column-wise with $\phi_i^\star=\arg\min_{\phi_i\in[0,2\pi)}\|\mathbf{x}_ie^{\mathrm{j}\phi_i}-\mathbf{x}_i^{\text{true}}\|_2^2$, for $i=1,...,I$, in the case

without temporal mixing. For the permutation ambiguity on $\mathbf{D}$ and $\mathbf{Z}$, a heuristic method is used to find the permutation that best matches the ground-truth with respect to the normalized cross correlation between columns in $\mathbf{D}$ and $\mathbf{D}^{\text{true}}$. After permutation, the estimation quality of $\mathbf{D}$ is evaluated by the minimum normalized squared error (MNSE) defined as $\mathrm{MNSE}(\mathbf{D})=\min_{\{\alpha_p\in\mathbb{C}\}_{p=1}^P}\left(\sum_{p=1}^P\|\alpha_p\mathbf{d}_p-\mathbf{d}_p^{\text{true}}\|_2^2\right)/\|\mathbf{D}^{\text{true}}\|_{\mathrm{F}}^2$. As for $\mathbf{Z}$, after permutation, we first perform the same global phase shift $e^{\mathrm{j}\phi^\star}$ on $\mathbf{Z}$ or $e^{\mathrm{j}\phi_i^\star}$ on each column $\mathbf{z}_i$ and then, the MNSE of $\mathbf{Z}$ is analogously calculated as $\mathrm{MNSE}(\mathbf{Z})=\min_{\{\beta_p\in\mathbb{C}\}_{p=1}^P}\left(\sum_{p=1}^P\|\beta_p\mathbf{z}_{p:}-\mathbf{z}_{p:}^{\text{true}}\|_2^2\right)/\|\mathbf{Z}^{\text{true}}\|_{\mathrm{F}}^2$. Moreover, the accuracy of the support of the estimated $\mathbf{Z}$ is evaluated by F-measure$=2\mathrm{TP}/(2\mathrm{TP}+\mathrm{FP}+\mathrm{FN})$, defined from the number of correctly and incorrectly estimated nonzeros: true positives (TP), false positives (FP), and false negatives (FN) [46].

B. Hyperparameter Choices

Sparsity Parameter of the cPRDL Problem in (3)**.** The solution for $\mathbf{Z}$ in problem (3) tends to $\mathbf{0}$ as $\lambda\rightarrow\infty$ and there exists an upper bound $\lambda_{\max}$ such that, for $\lambda\geq\lambda_{\max}$, any point with $\mathbf{Z}=\mathbf{0}$ is stationary for problem (3) [47]. With knowledge of $\lambda_{\max}$, the problem of searching for a suitable sparsity regularization parameter λ for an instance is significantly reduced, since any $\lambda\geq\lambda_{\max}$ is ineffective.

Using the stationarity conditions (27), we can derive the following upper bound:

$$\lambda_{\max}=\|\mathbf{Y}\|_{\mathrm{F}}\cdot\max_{i=1,...,I}\{\sigma_{\max}(\mathbf{F}_i)\}, \quad (52)$$

where $\sigma_{\max}(\cdot)$ denotes the largest singular value. For $\lambda\geq\lambda_{\max}$, any point $(\mathbf{D},\mathbf{0})$ with $\mathbf{D}\in\mathcal{D}$ is a stationary point of the original problem (3). Moreover, it is easy to verify that all points $(\mathbf{D},\mathbf{0})$ with $\mathbf{D}\in\mathcal{D}$ are equally optimal for problem (3).

For the three investigated particular cases of linear operator $\mathcal{F}$, the upper bound $\lambda_{\max}$ can be further decreased. In Case 1 and 2, where the spatial mixing is time-invariant and $\mathcal{F}$ reduces to the model (51), $\lambda_{\max}$ can be decreased to

$$\lambda_{\max}=\sigma_{\max}(\mathbf{A})\cdot\max_{i=1,...,I}\left\{\sum_{m=1}^{M_2}|b_{im}|\cdot\|\mathbf{y}_m\|_2\right\}. \quad (53)$$

Then, in Case 3, $\lambda_{\max}$ can be decreased to

$$\lambda_{\max}=\max_{i=1,...,I}\left\{\sigma_{\max}(\mathbf{A}_i)\cdot\|\mathbf{y}_i\|_2\right\}. \quad (54)$$

The intermediate derivations of the upper bounds $\lambda_{\max}$ in (52)-(54) can be found in Appendix D.

Regularization Parameters of the PRDL Problem in (4)**.** Problem (4) has two regularization parameters μ and ρ. Similar to λ in (3), ρ adjusts the sparsity level of matrix $\mathbf{Z}$, whereas

μ controls the trade-off between the data fidelity and the approximation quality of the sparse representation.

Similarly, for the sparsity parameter ρ in (4), there exists an upper bound $\rho_{\max}$ such that, for any $\rho \geq \rho_{\max}$, problem (4) always admits a stationary point with $\mathbf{Z}=\mathbf{0}$. From the stationarity conditions (41)-(42), we obtain an upper bound

$$\rho_{\max} = \frac{\mu \cdot \sigma_{\max}(\mathbf{F}) \cdot \|\mathbf{Y}\|_F}{\sigma_{\min}^2(\mathbf{F}) + \mu}. \tag{55}$$

$\sigma_{\min}(\cdot)$ denotes the smallest singular value, which may be zero.

Furthermore, in Case 1 and 3, where no temporal mixing is applied, each snapshot $\mathbf{x}_i$ is observed independently and, hence, the upper bound $\rho_{\max}$ can be decreased to

$$\rho_{\max} = \max_{i=1,\dots,I} \left\{ \frac{\mu \sigma_{\max}(\mathbf{A}_i)}{\sigma_{\min}^2(\mathbf{A}_i) + \mu} \cdot \|\mathbf{y}_i\|_2 \right\}. \tag{56}$$

Note that Case 1 can be viewed as a special case of Case 3 where $\mathbf{A}_i = \mathbf{A}$ for all snapshots. The derivations of the upper bounds $\rho_{\max}$ in (55)-(56) are provided in Appendix E.

Next, we analyze the effect of parameter μ. Using the vectorized expression in (2) for $\mathcal{F}$, we can also write the gradient of $\widehat{f}^{(t)}$ with respect to $\mathbf{X}$ in a vectorized form as

$$\nabla_{\mathrm{vec}(\mathbf{X})} \widehat{f}^{(t)}(\mathbf{X},\mathbf{D},\mathbf{Z}) = \left(\mathbf{F}^H \mathbf{F} + \mu \mathbf{I}_{NI}\right) \mathrm{vec}(\mathbf{X})$$
$$- \left(\mathbf{F}^H \mathrm{vec}(\mathbf{Y}^{(t)}) + \mu \mathrm{vec}(\mathbf{D}\mathbf{Z})\right).$$

Then, the stationarity condition (42) can be rewritten as

$$\mathrm{vec}(\mathbf{X}) = (\mathbf{F}^H \mathbf{F} + \mu \mathbf{I}_{NI})^{-1} \mathbf{F}^H \mathrm{vec}(\mathbf{Y}^{(t)})$$
$$+ \left(\tfrac{1}{\mu} \mathbf{F}^H \mathbf{F} + \mathbf{I}_{NI}\right)^{-1} \mathrm{vec}(\mathbf{D}\mathbf{Z}). \tag{57}$$

As can be seen from (57), μ offers some control over how much the value of $\mathrm{vec}(\mathbf{X})$ at a stationary point of $\widehat{h}^{(t)}$ is influenced by the data fitting solution $\mathbf{F}^\dagger \mathrm{vec}(\mathbf{Y}^{(t)})$ and the sparse representation $\mathrm{vec}(\mathbf{D}\mathbf{Z})$. Also, the trade-off depends on both μ and $\mathbf{F}^H \mathbf{F}$. Thus, we propose to set μ to be proportional to the smallest nonzero eigenvalue of $\mathbf{F}^H \mathbf{F}$, i.e., $\sigma_{\min,\mathrm{nz}}^2(\mathbf{F})$, where $\sigma_{\min,\mathrm{nz}}(\cdot)$ is the smallest nonzero singular value. However, a suitable ratio has to be found by experiments.

The above analysis suggests that we can set the sparsity parameter λ in (3) (ρ in (4)) to be $\lambda = r\lambda_{\max}$ ($\rho = r\rho_{\max}$) with some factor $r \in [0,1]$. The theoretical dependence between the suitable value of factor r and the other parameters, e.g., problem sizes, is unfortunately unknown. Hence, we choose factor r for each simulation setup and algorithm based on some preliminary experiments. In a practical application, the suitable value of factor r can similarly be learned from some training data, where the true values of the variables are known.

C. Computational Experiments

In the following, we evaluate the complexity and estimation accuracy of the proposed algorithms under various parameter setups, in comparison to SC-PRIME. The number of receive antennas is set to $N=64$. The algorithms are terminated when the minimum-norm subgradient has achieved the tolerance $\varepsilon = 10^{-5}$ or after a maximum number of 2000 iterations. A following debiasing step is performed with the same termination condition. By default, the SNR is 15 dB, the spatial over-sampling rate is $M_1/N=4$, and $I=16N$ time-slots are taken.
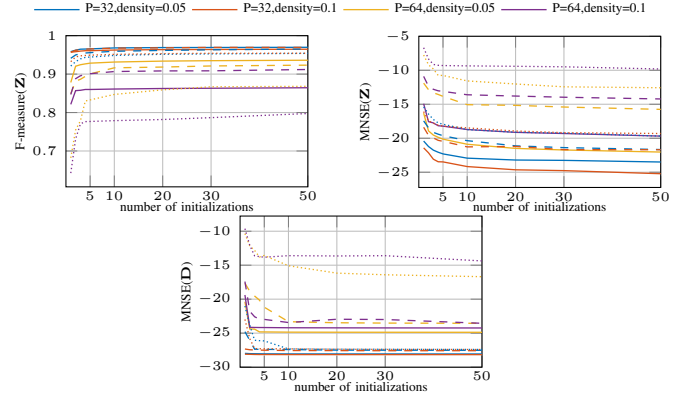

Fig. 3: Estimation quality vs. number of initializations using compact-SCAphase (solid), SCAphase (dashed), and SC-PRIME (dotted) in Case 1. $N=64, M_1=4N, I=16N$.
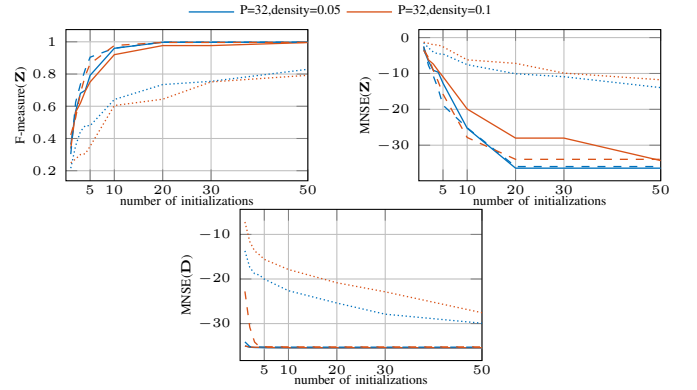

Fig. 4: Estimation quality vs. number of initializations using compact-SCAphase (solid), SCAphase (dashed), and SC-PRIME (dotted) in Case 2. $N=64, M_1=4N, I=16N$.

1) Case 1 – Time-invariant spatial mixing and no temporal mixing: We first consider the case without temporal mixing. The regularization parameters are set as follows. We set $\mu = \sigma_{\min,\mathrm{nz}}^2(\mathbf{F}) = \sigma_{\min,\mathrm{nz}}^2(\mathbf{A})$ for both SCAphase and SC-PRIME. The sparsity parameters are chosen to be $\lambda = 0.75^{16}\lambda_{\max}$ with $\lambda_{\max}$ calculated by (53) and $\rho = 0.75^{16}\rho_{\max}$ with $\rho_{\max}$ in (56) for compact-SCAphase and SCAphase, respectively. Although SC-PRIME adopts the same formulation, i.e., problem (4), as SCAphase, it typically requires a larger sparsity parameter ρ for achieving a good solution, due to the loose majorization on the data fitting term employed in the surrogate subproblems. Thus, for SC-PRIME, ρ is set to be $0.75^{15}\rho_{\max}$ and $0.75^{14}\rho_{\max}$ in the cases with $P=N/2$ and $P=N$, respectively.

Varying sparsity level. In the first simulation, as depicted in Fig. 2, the performance of the algorithms is evaluated for various choices of $\{P, L/P\}$. The number of users P is varied in $\{N/2, N\}$, and the density of active users in each time-slot, i.e., L/P, is limited to be $\{0.025, 0.05, 0.1, 0.2, 0.4\}$. As both problems (3) and (4) are nonconvex, multiple random initializations are used to increase the chance of finding the global optimal solution. Specifically, for each Monte Carlo trial, 10 initializations are performed, and the best reconstructed signal,
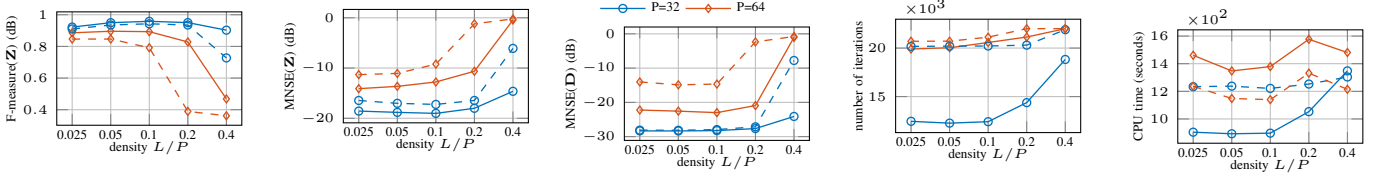
Fig. 5: Performance vs. density L/P using SCAphase (solid) and SC-PRIME (dashed) in Case 3. $N{=}64, M_1{=}4N, I{=}16N$.

determined by the lowest objective function value, is retained and further improved by a debiasing step. The total number of iterations and computational time, including that of the debiasing step, are reported in Fig. 2. The robustness of the algorithms to initialization is investigated afterwards in Fig. 3.

From Fig. 2, it can be observed that sparse channel access is required, i.e., a small value of L/P, for all algorithms to achieve good recovery performance. However, in the extremely sparse case, the received signals $\mathbf{X}^{\text{true}}{=}\mathbf{D}^{\text{true}}\mathbf{Z}^{\text{true}}$ contain only few linear combinations of columns of spatial signature $\mathbf{D}^{\text{true}}$, which results in a degradation of estimation qualities. Furthermore, for all choices of $\{P,L/P\}$, SC-PRIME does not converge within 2000 iterations. The solution obtained by SC-PRIME within 2000 iterations can be improved by using a larger sparsity parameter ρ than that in SCAphase, as in the parameter setup of this simulation. However, in Fig. 2, SC-PRIME still exhibits the poorest accuracy performance for most choices of $\{P,L/P\}$, compared to the other algorithms.

In Fig. 2, when $P{=}N/2$, all algorithms show good recovery performance, whereas compact-SCAphase and SCAphase exhibit faster convergence. Moreover, compared to SCAphase, compact-SCAphase uses half the number of iterations to attain a stationary point. However, the reduction of CPU time achieved by compact-SCAphase is not as significant as the reduced number of iterations because, as discussed in Section V-B, compact-SCAphase has the highest per-iteration complexity. In contrast, when the number of users is comparable to that of antennas, i.e., $P{=}N$, only compact-SCAphase achieves the given tolerance within 2000 iterations. This is intuitive as in the regime of $P{\geq}N$, and with sparse channel access, the information of the users' channels contained in the measurements is insufficient. To resolve this challenge, a higher spatial oversampling rate is required. Nevertheless, compared to SC-PRIME, compact-SCAphase and SCAphase show a significant improvement of estimation accuracy. Then, compared to SCAphase, compact-SCAphase further improves the estimation quality of $\mathbf{Z}$ due to fast convergence.

Varying number of initializations. In the second simulation, we investigate the robustness of the algorithms to initialization. The performance behavior of the algorithms with the number of random initializations varied from 1 to 50 is presented in Fig. 3. The number of users P and density are set to be $\{N/2,N\}$ and $\{0.05,0.1\}$, respectively. In Fig. 3, for most choices of $\{P,L/P\}$, all algorithms show similar robustness to initialization as the estimation quality achieved by each algorithm remains constant after the trial of 10 initializations, and compact-SCAphase possesses the lowest estimation errors. In the cases with $P{=}N$, SC-PRIME shows a significant degra-

dation on the estimation quality compared to the proposed algorithms, which, as demonstrated in Fig. 2, results from the fact that SC-PRIME generally does not converge within the limit of 2000 iterations. Additionally, if only the spatial signature $\mathbf{D}$ needs to be recovered, then 5 initializations are sufficient for all algorithms to attain a good estimation accuracy. Particularly, when $P{=}N/2$, compact-SCAphase achieves a good stationary point for $\mathbf{D}$ even with a single initialization.

2) Case 2 – Time-invariant spatial mixing and STFT temporal mixing: Next, a temporal mixing network that performs the same STFT independently on each output channel of the spatial mixing network is introduced (see [16] for more details of the STFT measurement model). For the STFT, we use an I-point DFT, a rectangular window of length $I/2$, a hop size of $I/4$. The above parameter setup results in a temporal oversampling rate of 5. Similar to the previous simulation, in Fig. 4, the estimation accuracy of the algorithms is evaluated as a function of number of initializations. We set $P{=}N/2$ and density $L/P{=}\{0.05,0.1\}$. The regularization parameters are chosen to be $\lambda{=}0.75^{25}\lambda_{\max}, \mu{=}\sigma^2_{\min,\text{nz}}(\mathbf{F}){=}\sigma^2_{\min,\text{nz}}(\mathbf{A})\sigma^2_{\min,\text{nz}}(\mathbf{B})$, and $\rho{=}0.75^{28}\rho_{\max}$ and $\rho{=}0.75^{23}\rho_{\max}$ for SCAphase and SC-PRIME, respectively, with $\rho_{\max}$ in (55).

Comparing the results in Fig. 3 and 4, we observe that, given a sufficient number of initializations, the estimation qualities are significantly improved in the case with STFT temporal mixing due to the increase of overall sampling rate. However, all algorithms become less robust to initialization. In particular, compact-SCAphase and SCAphase require 20 initializations to attain a good stationary point, whereas SC-PRIME cannot achieve the same estimation accuracy as the other algorithms even with 50 initializations since, as we discussed, SC-PRIME does not converge within 2000 iterations.

3) Case 3 – Time-variant spatial mixing and no temporal mixing: As discussed in Section V-B, compared to the other two algorithms, compact-SCAphase has a per-iteration complexity of higher order in the general case with a linear measurement operator $\mathcal{F}$ in (49) with multiple chains of mixing networks. Therefore, in the case with time-variant spatial mixing, we only compare SCAphase with SC-PRIME, as the running time of compact-SCAphase is unaffordable. As depicted in Fig. 5, the accuracy and complexity of the algorithms are evaluated for various choices of $\{P,L/P\}$. All parameters are the same as in Fig. 2, except that the spatial mixing $\mathbf{A}_i$ for each snapshot is generated independently.

What stands out in Fig. 5 is that the use of time-variant spatial mixing overcomes the challenge of lack of diversity in the extremely sparse case observed in Fig. 2. On the other hand, the convergence rates of the two algorithms measured

by number of iterations in Fig. 5 are similar to that in Fig. 2. However, due to the increased complexity of linear operator $\mathcal{F}$, the two algorithms possess similar per-iteration complexity. Hence, compared to SC-PRIME, SCAphase exhibits a significantly improved convergence rate in terms of both number of iterations and computational time, when $P=N/2$.

VII. CONCLUSION

In this paper, we introduce an extension of SCA framework for the phase retrieval with dictionary learning problem. Two efficient parallel algorithms are proposed by applying the extended SCA framework to two complementary formulations, respectively. The first algorithm, termed *compact-SCAphase*, employs a compact ℓ_1-regularized nonconvex LS formulation, which avoids the auxiliary variables required in state-of-the-art methods such as SC-PRIME and DOLPHIn. The second algorithm, denoted by *SCAphase*, solves the conventional formulation as in SC-PRIME. An efficient procedure based on rational approximation is devised for solving the ℓ_2-norm constrained LS subproblems under the SCA framework. For both algorithms, we refined the search range for suitable values of the sparsity parameter. Simulation results on synthetic data in the context of blind channel estimation in multi-antenna random access network demonstrate the fast convergence of SCAphase compared to SC-PRIME. Moreover, compact-SCAphase is more competitive than SCAphase in terms of both computational complexity and parameter tuning cost in the case with less diverse linear measurement operators. Nevertheless, SCAphase also has several advantages over compact-SCAphase. Compared to SCAphase, the computational complexity of compact-SCAphase dramatically grows with the increase of diversity of the designed linear measurement operator. Also, SCAphase can easily include potential side constraints on the signal of interest.

Several questions that have been answered for the classic phase retrieval remain open for phase retrieval with dictionary learning. First, further work needs to be done to establish the theoretical conditions for a guaranteed unique recovery (up to trivial ambiguities) of the dictionary and/or the sparse codes. Moreover, the simulation results in Section VI show that multiple random initializations are required for attaining (near-)global minima of our nonconvex formulations. Therefore, it is of great interest to develop a more sophisticated initialization strategy that can help avoid poor stationary points.

APPENDIX A
SOLUTION APPROACH FOR SUBPROBLEM (12)

In the following, we derive the solution approach for subproblem (12) that involves vector $\mathbf{d}_p$ by solving the KKT optimality system, since the strong duality holds for (12).

The gradient of $L(\mathbf{d}_p, \nu_p)$ in (14) with respect to $\mathbf{d}_p$ is

$$\nabla_{\mathbf{d}_p} L(\mathbf{d}_p, \nu_p) = \left(\mathbf{H}_p^{\mathrm{H}} \mathbf{H}_p + \nu_p \mathbf{I}_N \right) \mathbf{d}_p - \mathbf{H}_p^{\mathrm{H}} \mathrm{vec}(\mathbf{Y}_p^{(t)}).$$

Then, the primal and dual optimal solutions must satisfy the following KKT system:

$$\nabla_{\mathbf{d}_p} L(\mathbf{d}_p, \nu_p) = \mathbf{0}, \qquad \text{(stationarity)} \qquad (58a)$$

$$\|\mathbf{d}_p\|_2^2 \leq 1, \nu_p \geq 0, \qquad \text{(primal and dual feasibility)} \qquad (58b)$$

$$\nu_p(\|\mathbf{d}_p\|_2^2 - 1) = 0. \qquad \text{(complementary slackness)} \qquad (58c)$$

For notational simplicity, we omit the iteration index t and let $\widetilde{\mathbf{d}}_p$ and $\widetilde{\nu}_p$ denote any pair of primal and dual optimal solutions in the derivations below. Two mutually exclusive possibilities arise due to (58b): a) $\widetilde{\nu}_p = 0$, or b) $\widetilde{\nu}_p > 0$.

Given dual variable $\nu_p = 0$, the solution $\mathbf{d}_p^{(\nu_p=0)}$ of (58a) corresponds to a solution of problem (12) when the ℓ_2-norm constraint is ignored. It is expressed as follows:

$$\mathbf{d}_p^{(\nu_p=0)} = (\mathbf{H}_p^{\mathrm{H}} \mathbf{H}_p)^\dagger \mathbf{H}_p^{\mathrm{H}} \mathrm{vec}(\mathbf{Y}_p^{(t)}). \qquad (59)$$

If $\mathbf{H}_p$ has full column rank, i.e., $\mathrm{rank}(\mathbf{H}_p) = N$, $\mathbf{d}_p^{(\nu_p=0)}$ is the unique solution of (58a). Otherwise, $\mathbf{d}_p^{(\nu_p=0)}$ is the solution with minimum ℓ_2-norm. In both cases above, if $\|\mathbf{d}^{(\nu_p=0)}\|_2 \leq 1$, then all conditions in (58) are fulfilled and, consequently, $\widetilde{\nu}_p = 0$ and $\widetilde{\mathbf{d}}_p = \mathbf{d}_p^{(\nu_p=0)}$ is a pair of optimal solutions.

However, if $\mathbf{d}^{(\nu_p=0)}$ does not satisfy the primal constraint, then $\widetilde{\nu}_p > 0$ must hold. Let $\mathbf{H}_p = \mathbf{U}\boldsymbol{\Sigma}\mathbf{V}^{\mathrm{H}}$ be the SVD of $\mathbf{H}_p$ and $\sigma_1 \geq ... \geq \sigma_r > 0$ be the non-zero singular values with $r = \mathrm{rank}(\mathbf{H}_p)$. Then, for $\nu_p > 0$, the stationarity condition (58a) can be rewritten as

$$\mathbf{d}_p = \mathbf{V}(\boldsymbol{\Sigma}^{\mathrm{H}}\boldsymbol{\Sigma} + \nu_p \mathbf{I}_N)^{-1}\boldsymbol{\Sigma}^{\mathrm{H}}\mathbf{U}^{\mathrm{H}}\mathrm{vec}(\mathbf{Y}_p^{(t)}). \qquad (60)$$

Thus, the squared ℓ_2-norm of $\mathbf{d}_p$ that satisfies condition (60) is a function of ν_p, which we define as $\psi_p(\nu_p) = \|\mathbf{d}_p\|_2^2$. Defining

$$\mathbf{c}_p = \boldsymbol{\Sigma}^{\mathrm{H}}\mathbf{U}^{\mathrm{H}}\mathrm{vec}(\mathbf{Y}_p^{(t)}), \qquad (61)$$

function $\psi_p(\nu_p)$ can be explicitly written as a rational function:

$$\psi_p(\nu_p) = \sum_{i=1}^r \frac{|c_{ip}|^2}{(\sigma_i^2 + \nu_p)^2}, \quad \text{for } \nu_p > 0, \qquad (62)$$

where c_{ip} is the i-th element of vector $\mathbf{c}_p$. Although (62) is derived for $\nu_p > 0$, the expression also holds for $\nu_p = 0$, i.e., $\psi_p(0) = \|\mathbf{d}_p^{(\widetilde{\nu}_p=0)}\|_2^2$, which is assumed to be above one in the present case b). Then, due to (58c), $\widetilde{\nu}_p$ coincides with the unique solution of $\psi_p(\nu_p) = 1$ in $(0, +\infty)$. Consequently, the optimal solution $\widetilde{\mathbf{d}}_p$ is obtained by substituting $\widetilde{\nu}_p$ into (60).

In conclusion, for $p=1,...,P$, the dual optimal points $\widetilde{\nu}_p$ are determined independently by the following rule:

$$\widetilde{\nu}_p \begin{cases} =0, & \text{if } \psi_p(0) \leq 1, \\ \in \{\nu_p > 0 | \psi_p(\nu_p) = 1\}, & \text{if } \psi_p(0) > 1. \end{cases}$$

Then, combining (59) and (60) and exploiting the SVD of matrix $\mathbf{H}_p$ to further reduce the complexity, we express the optimal solution $\widetilde{\mathbf{d}}_p$ to problem (12) as

$$\widetilde{\mathbf{d}}_p = \mathbf{V}(\boldsymbol{\Sigma}^{\mathrm{H}}\boldsymbol{\Sigma} + \widetilde{\nu}_p \mathbf{I}_N)^\dagger \mathbf{c}_p.$$

For the particular linear operator $\mathcal{F}$ in (51), the SVD of $\mathbf{H}_p$ in (13) can be calculated analytically given the SVD of $\mathbf{A}$. In this case, the corresponding matrix $\mathbf{F}$ in the vectorized form is

$$\mathbf{F} = \mathbf{B}^{\mathrm{T}} \otimes \mathbf{A}. \qquad (63)$$

Thus, $\mathbf{H}_p$ can be written as $\mathbf{H}_p = (\mathbf{B}^{\mathrm{T}} \otimes \mathbf{A}) \cdot (\mathbf{z}_{p:}^{(t)} \otimes \mathbf{I}_N) = (\mathbf{B}^{\mathrm{T}}\mathbf{z}_{p:}^{(t)}) \otimes \mathbf{A}$. Further, let $\mathbf{A} = \mathbf{U}_A \boldsymbol{\Sigma}_A \mathbf{V}_A^{\mathrm{H}}$ and $\mathbf{B}^{\mathrm{T}}\mathbf{z}_{p:}^{(t)} = \mathbf{U}_B \boldsymbol{\Sigma}_B \mathbf{V}_B^{\mathrm{H}}$ be the compact SVDs of $\mathbf{A}$ and $\mathbf{B}^{\mathrm{T}}\mathbf{z}_{p:}^{(t)}$, respectively. Then, the
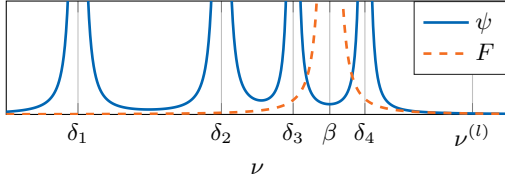
Fig. 6: Original and approximate rational functions, $r=4$

compact SVD of $\mathbf{H}_p$ can be expressed as [38]:

$$\mathbf{H}_p=\underbrace{(\mathbf{U}_A\otimes\mathbf{U}_B)}_{\mathbf{U}}\underbrace{(\boldsymbol{\Sigma}_A\otimes\boldsymbol{\Sigma}_B)}_{\boldsymbol{\Sigma}}\underbrace{(\mathbf{V}_A\otimes\mathbf{V}_B)^{\mathrm{H}}}_{\mathbf{V}^{\mathrm{H}}}.$$

As a column vector, $\mathbf{B}^{\mathrm{T}}\mathbf{z}_{p:}^{(t)}$ has $\mathbf{V}_B=1$ and only one nonzero singular value $\|\mathbf{B}^{\mathrm{T}}\mathbf{z}_{p:}^{(t)}\|_2$. Therefore, the nonzero singular values of $\mathbf{H}_p$ are given by $\|\mathbf{B}^{\mathrm{T}}\mathbf{z}_{p:}^{(t)}\|_2\cdot\sigma_i^A$, for $i=1,...,r$, where $\{\sigma_i^A\}_{i=1}^r$ are the nonzero singular values of $\mathbf{A}$ and $r=\mathrm{rank}(\mathbf{H}_p)=\mathrm{rank}(\mathbf{A})$. Moreover, due to $\mathbf{V}_B=1$, we have

$$\mathbf{U}\boldsymbol{\Sigma}=(\mathbf{U}_A\boldsymbol{\Sigma}_A)\otimes(\mathbf{U}_B\boldsymbol{\Sigma}_B)=(\mathbf{U}_A\boldsymbol{\Sigma}_A)\otimes\big(\mathbf{B}^{\mathrm{T}}\mathbf{z}_{p:}^{(t)}\big).$$

Consequently, vector $\mathbf{c}_p$ defined in (61) can be written as

$$\mathbf{c}_p=(\mathbf{U}_A\boldsymbol{\Sigma}_A)^{\mathrm{H}}\otimes(\mathbf{B}^{\mathrm{T}}\mathbf{z}_{p:}^{(t)})^{\mathrm{H}}\mathrm{vec}(\mathbf{Y}_p^{(t)})=\boldsymbol{\Sigma}_A^{\mathrm{H}}\mathbf{U}_A^{\mathrm{H}}\mathbf{Y}_p^{(t)}\mathbf{B}^{\mathrm{H}}\bar{\mathbf{z}}_{p:}^{(t)}.$$

Finally, after having obtained the dual optimal solution $\tilde{\nu}_p$ by the same procedure as described in Section III, we can also compute the optimal solution $\tilde{\mathbf{d}}_p$ using the SVD of $\mathbf{A}$:

$$\tilde{\mathbf{d}}_p=\mathbf{V}_A\left(\boldsymbol{\Sigma}_A^{\mathrm{H}}\boldsymbol{\Sigma}_A+\tilde{\nu}_p\mathbf{I}_r\right)^{\dagger}\mathbf{c}_p.$$

APPENDIX B
PROOF OF THEOREM 1

The original rational function $\psi(\nu)$ in (16) and its derivative $\psi'(\nu)$ can be rewritten as

$$\psi(\nu)=\sum_{i=1}^r\frac{|c_i|^2}{(\delta_i-\nu)^2}\quad\text{and}\quad\psi'(\nu)=\sum_{i=1}^r\frac{2|c_i|^2}{(\delta_i-\nu)^3},$$

with the poles $\delta_1\leq...\leq\delta_r<0$. We ignore the trivial case where all poles δ_i are identical. Let $\zeta(\nu)=F(\nu;\alpha,\beta)-\psi(\nu)$ with the approximate function F defined in (24). It is sufficient to show that $\zeta(\nu)<0$ for $\nu>\delta_r,\nu\neq\nu^{(l)}$. To this end, define

$$\xi(\nu)=\zeta(\nu)(\beta-\nu)^2\prod_{i=1}^r(\delta_i-\nu)^2.$$

Then, ξ is a polynomial of degree $2r$ with real coefficients:

$$\xi(\nu)=\alpha\prod_{i=1}^r(\delta_i-\nu)^2-(\beta-\nu)^2\sum_{i=1}^r|c_i|^2\prod_{j=1,j\neq i}^r(\delta_j-\nu)^2. \quad (64)$$

The product rule for differentiation determines that $\xi(\nu^{(l)})=0$ and its derivative $\xi'(\nu^{(l)})=0$ since $\zeta(\nu^{(l)})=0$ and its derivative $\zeta'(\nu^{(l)})=0$. Hence, $\nu^{(l)}$ is a double root of ξ, and we can extract the factor $(\nu-\nu^{(l)})^2$ and rewrite (64) as

$$\xi(\nu)=\left(\alpha-\sum_{i=1}^r|c_i|^2\right)(\nu-\nu^{(l)})^2\prod_{i=1}^{r-1}(\nu^2-2a_i\nu+b_i),$$

with appropriately chosen coefficients $a_i,b_i\in\mathbb{R}$.

We claim that $\nu^{(l)}$ is the only real double root of ξ in the interval $(\delta_r,+\infty)$. To see this, observe from (25) that

$$\beta=\frac{2}{\psi'(\nu^{(l)})}\sum_{i=1}^r\frac{\delta_i|c_i|^2}{(\delta_i-\nu^{(l)})^3}.$$

Thus, it is easy to verify that $\delta_1<\beta<\delta_r<0$. The roots of ζ are also the roots of ξ. The following result can be intuitively

observed from Fig. 6. Each interval (δ_i,δ_{i+1}) with $\delta_i\neq\delta_{i+1}$ contains either two real roots of ζ or the real part of a pair of complex conjugate roots. In contrast, if $\delta_i=\delta_{i+1}$ for some $i=1,...,r-1$, it can be trivially identified from (64) that δ_i is a double root of ξ. Therefore, the real parts of all the remaining $2r-2$ roots of ξ fall in the interval $[\delta_1,\delta_r]$. The claim is established; it can be proved more formally by factorizing (64).

This argument shows that $\mathrm{sign}(\xi(\nu))$ remains constant in $[\delta_r,\nu^{(l)})\cup(\nu^{(l)},+\infty)$. Hence, it follows from (64) that, for all $\nu>\delta_r,\nu\neq\nu^{(l)}$, $\mathrm{sign}(\zeta(\nu))=\mathrm{sign}(\xi(\nu))=\mathrm{sign}(\xi(\delta_r))=-1$. This implies that $F(\nu;\alpha,\beta)<\psi(\nu)$ for all $\nu>\delta_r,\nu\neq\nu^{(l)}$. ∎

APPENDIX C
PROOF OF THEOREM 3

In this paper, Algorithm 1 and Algorithm 3 are developed for the phase retrieval with dictionary learning problem. However, this framework can be easily generalized to another nonconvex nonsmooth problem with a locally Lipschitz objective function, and the convergence is ensured under several assumptions on the approximate functions. Therefore, in the following, we first demonstrate the convergence of the generalized algorithm for the general constrained problem (46). Then, we verify that the required assumptions are satisfied in the compact-SCAphase algorithm and, thus, Theorem 3 can be proved. In the following analysis, for simplicity, we ignore the convex nonsmooth regularization, e.g., the ℓ_1-regularization in (3). However, a regularized problem can be written in the standard form (46) with the reformulation in [29, Eq. (18)] and, then, the analysis below can be directly applied.

Let $\hat{f}^{(t)}(\mathbf{s})$ be a smooth majorizing function of f in (46) at $\mathbf{s}^{(t)}$ and $\tilde{f}^{(t)}(\mathbf{s})$ be a pseudoconvex approximation of $\hat{f}^{(t)}$ at $\mathbf{s}^{(t)}$ in the generalized algorithm. Precisely, $\hat{f}^{(t)}$ and $\tilde{f}^{(t)}$ are constructed to satisfy the following assumptions:

(A1) $\tilde{f}^{(t)}(\mathbf{s})$ is pseudoconvex in $\mathbf{s}$ for any $\mathbf{s}\in\mathcal{C}$;

(A2) $\tilde{f}^{(t)}(\mathbf{s})$ and $\hat{f}^{(t)}(\mathbf{s})$ are C^1-smooth in $\mathcal{C}$;

(A3) $\hat{f}^{(t)}(\mathbf{s})\geq f(\mathbf{s})$ for all $\mathbf{s}\in\mathcal{C}$ and $\hat{f}^{(t)}(\mathbf{s}^{(t)})=f(\mathbf{s}^{(t)})$;

(A4) $\nabla\tilde{f}^{(t)}(\mathbf{s}^{(t)})=\nabla\hat{f}^{(t)}(\mathbf{s}^{(t)})\in\partial_C f(\mathbf{s}^{(t)})$.

Then, under Assumptions (A1)-(A4), the solution sequence obtained by the generalized algorithm converges to a relaxed C-stationary point of problem (46). The proof is as follows. The convergence analyses of the MM algorithms [32] and the SCA framework [29] for a smooth function f are actually equivalent as they both rely on the two essential facts, namely the descent property $f(\mathbf{s}^{(t+1)})\leq f(\mathbf{s}^{(t)})$ and the gradient consistency between the original function and its approximation, which ensures that every fixed-point of the algorithm is a stationary point of the original problem. In a similar way, we can establish the convergence of our proposed algorithm. First, Assumptions (A1), (A2), and (A4) ensure that the minimizer of $\tilde{f}^{(t)}$ indicates a descent direction of the majorizing function $\hat{f}^{(t)}$. Then, a decrease of the original function f is achieved in our proposed algorithm by exact line search on $\hat{f}^{(t)}$ along this descent direction:

$$f(\mathbf{s}^{(t+1)})\leq\hat{f}^{(t)}(\mathbf{s}^{(t+1)})\leq\hat{f}^{(t)}(\mathbf{s}^{(t)})\leq f(\mathbf{s}^{(t)}). \quad (65)$$

Second, from the smoothness assumption (A2) and the subgradient consistency assumption (A4), we have $\partial_C \widetilde{f}^{(t)}(\mathbf{s}^{(t)}) = \{\nabla \widetilde{f}^{(t)}(\mathbf{s}^{(t)})\}$ and $\partial_C \widehat{f}^{(t)}(\mathbf{s}^{(t)}) = \{\nabla \widehat{f}^{(t)}(\mathbf{s}^{(t)})\}$ [43], and then

$$\partial_C \widetilde{f}^{(t)}(\mathbf{s}^{(t)}) + \partial_C \mathbb{I}_C(\mathbf{s}^{(t)}) = \partial_C \widehat{f}^{(t)}(\mathbf{s}^{(t)}) + \partial_C \mathbb{I}_C(\mathbf{s}^{(t)})$$
$$\subseteq \partial_C f(\mathbf{s}^{(t)}) + \partial_C \mathbb{I}_C(\mathbf{s}^{(t)}). \quad (66)$$

By the definition of relaxed C-stationarity in (47), property (66) guarantees that every fixed-point of the generalized algorithm is a relaxed C-stationary point of the majorization and the original problem (46). Finally, based on properties (65) and (66), the convergence to a relaxed C-stationary point of problem (46) can be easily demonstrated by following the same line of analysis as in [29], [32].

Now, to prove Theorem 3, we only need to justify that Assumptions (A1)-(A4) are satisfied in the compact-SCAphase algorithm that solves problem (3). As mentioned at the beginning of this section, for simplicity, the ℓ_1-regularization is discarded and only the nonsmooth LS function f in (5) is minimized. First, as can be trivially verified, the original function f in (5) is locally Lipschitz, the feasible set in (3) is closed and convex, and the smooth majorizing function $\widehat{f}^{(t)}$ in (7) and the convex approximation $\widetilde{f}^{(t)} = \widetilde{f}_D^{(t)} + \widetilde{f}_Z^{(t)}$ in (9) satisfy Assumptions (A1)-(A3). Then, the remaining subgradient consistency assumption (A4) is verified as follows. The gradient consistency between the majorizing function $\widehat{f}^{(t)}$ and the convex approximation $\widetilde{f}^{(t)}$ is directly ensured by the best-response approximation. If f is differentiable at $(\mathbf{D}^{(t)}, \mathbf{Z}^{(t)})$, the majorization enforces the gradient consistency between f and the smooth majorizing function $\widehat{f}^{(t)}$. Thus, we have

$$\nabla \widetilde{f}^{(t)}(\mathbf{D}^{(t)}, \mathbf{Z}^{(t)}) = \nabla \widehat{f}^{(t)}(\mathbf{D}^{(t)}, \mathbf{Z}^{(t)}) = \nabla f(\mathbf{D}^{(t)}, \mathbf{Z}^{(t)})$$

and, hence, Assumption (A4) is trivially satisfied. Otherwise, at a non-differentiable point $(\mathbf{D}^{(t)}, \mathbf{Z}^{(t)})$ of f, we have

$$\nabla \widetilde{f}^{(t)}(\mathbf{D}^{(t)}, \mathbf{Z}^{(t)}) = \nabla \widehat{f}^{(t)}(\mathbf{D}^{(t)}, \mathbf{Z}^{(t)})$$
$$\in \partial_B f(\mathbf{D}^{(t)}, \mathbf{Z}^{(t)}) \subseteq \partial_C f(\mathbf{D}^{(t)}, \mathbf{Z}^{(t)}), \quad (67)$$

which is proven as follows. First, note that f in (5) is non-differentiable only at the points $(\mathbf{D}, \mathbf{Z})$ where the output of the linear operator $\mathcal{F}(\mathbf{D}\mathbf{Z})$ contains zero entries. Since 0 has undetermined phase, in the implementation, if $(\mathbf{D}^{(t)}, \mathbf{Z}^{(t)})$ is a non-differentiable point of f, we have to assign some specific phases to the zero entries of $\mathcal{F}(\mathbf{D}^{(t)}\mathbf{Z}^{(t)})$ in order to construct a smooth majorization $\widehat{f}^{(t)}$. Now assume that we have assigned specific phases to the zero entries of $\mathcal{F}(\mathbf{D}^{(t)}\mathbf{Z}^{(t)})$ and the phases are denoted by $\arg\left(\mathcal{F}(\mathbf{D}^{(t)}\mathbf{Z}^{(t)})\right)$. Then, the majorizing function $\widehat{f}^{(t)}$ is tight not only at $(\mathbf{D}^{(t)}, \mathbf{Z}^{(t)})$ but also at any point $(\mathbf{D}, \mathbf{Z})$ with $\arg(\mathcal{F}(\mathbf{D}\mathbf{Z})) = \arg\left(\mathcal{F}(\mathbf{D}^{(t)}\mathbf{Z}^{(t)})\right)$, i.e., $\widehat{f}^{(t)}(\mathbf{D}, \mathbf{Z}) = f(\mathbf{D}, \mathbf{Z})$ for all $(\mathbf{D}, \mathbf{Z})$ with $\arg(\mathcal{F}(\mathbf{D}\mathbf{Z})) = \arg\left(\mathcal{F}(\mathbf{D}^{(t)}\mathbf{Z}^{(t)})\right)$. As discussed earlier, the upper bound property enforces the gradient consistency between f and $\widehat{f}^{(t)}$ at any differentiable point of f where the upper bound is tight. Therefore, we have

$$\nabla \widehat{f}^{(t)}(\mathbf{D}, \mathbf{Z}) = \nabla f(\mathbf{D}, \mathbf{Z}) \text{ for all } (\mathbf{D}, \mathbf{Z}) \in \mathcal{S} \text{ with}$$

$$\mathcal{S} = \left\{ (\mathbf{D}, \mathbf{Z}) \Big|_{[\mathcal{F}(\mathbf{D}\mathbf{Z})]_{kl} \neq 0, \forall k=1,\dots,M_1, l=1,\dots,M_2}^{\arg(\mathcal{F}(\mathbf{D}\mathbf{Z})) = \arg(\mathcal{F}(\mathbf{D}^{(t)}\mathbf{Z}^{(t)}))} \right\}. \quad (68)$$

The current point $(\mathbf{D}^{(t)}, \mathbf{Z}^{(t)})$ is an accumulation point of $\mathcal{S}$ since the linear operator $\mathcal{F}$ is a continuous map. Then, as $\widehat{f}^{(t)}$

is a quadratic function, which is C^1-smooth, we have

$$\lim_{\substack{(\mathbf{D}, \mathbf{Z}) \in \mathcal{S}, \\ (\mathbf{D}, \mathbf{Z}) \to (\mathbf{D}^{(t)}, \mathbf{Z}^{(t)})}} \nabla f(\mathbf{D}, \mathbf{Z}) = \lim_{\substack{(\mathbf{D}, \mathbf{Z}) \in \mathcal{S}, \\ (\mathbf{D}, \mathbf{Z}) \to (\mathbf{D}^{(t)}, \mathbf{Z}^{(t)})}} \nabla \widehat{f}^{(t)}(\mathbf{D}, \mathbf{Z})$$
$$= \nabla \widehat{f}^{(t)}(\mathbf{D}^{(t)}, \mathbf{Z}^{(t)}). \quad (69)$$

Finally, by the definitions of generalized subdifferentials in (44) and (45), we conclude from (69) that $\nabla \widehat{f}^{(t)}(\mathbf{D}^{(t)}, \mathbf{Z}^{(t)})$ is an element of $\partial_B f(\mathbf{D}^{(t)}, \mathbf{Z}^{(t)})$ and, consequently, also an element of $\partial_C f(\mathbf{D}^{(t)}, \mathbf{Z}^{(t)})$. Intuitively speaking, the smooth majorization $\widehat{f}^{(t)}$ retains the directional derivatives of f towards the directions in which the phases of the output of the mixing network $\arg(\mathcal{F}(\mathbf{D}\mathbf{Z}))$ remain the same as that at $(\mathbf{D}^{(t)}, \mathbf{Z}^{(t)})$. Thus, we have verified that Assumptions (A1)-(A4) are satisfied in the compact-SCAphase algorithm and, therefore, the solution sequence generated by compact-SCAphase converges to a relaxed C-stationary point of problem (3). ∎

APPENDIX D
DERIVATION OF UPPER BOUND $\lambda_{\max}$

We derive the upper bound $\lambda_{\max}$ for the sparsity parameter λ in (3) using the stationarity conditions (27) with the gradients given in (8). Condition (27a) is trivial for $\mathbf{Z} = \mathbf{0}$ as $\nabla_{\mathbf{D}} \widehat{f}^{(t)}(\mathbf{D}, \mathbf{0}) = \mathbf{0}$ for any $\mathbf{D}$. Then, adopting the vectorized expression in (2) for $\mathcal{F}$ and the partitioning in (21), we can write the gradient $\nabla_{z_{pi}} \widehat{f}^{(t)}$ at $\mathbf{Z} = \mathbf{0}$ as $\nabla_{z_{pi}} \widehat{f}^{(t)}(\mathbf{D}, \mathbf{0}) = -\mathbf{d}_p^{\mathrm{H}} \mathbf{F}_i^{\mathrm{H}} \mathrm{vec}(\mathbf{Y}^{(t)})$. It leads to the following inequality:

$$|\nabla_{z_{pi}} \widehat{f}^{(t)}(\mathbf{D}, \mathbf{0})| \leq \|\mathbf{d}_p\|_2 \|\mathbf{F}_i^{\mathrm{H}} \mathrm{vec}(\mathbf{Y}^{(t)})\|_2 \quad (70\text{a})$$
$$\leq \|\mathbf{F}_i^{\mathrm{H}} \mathrm{vec}(\mathbf{Y}^{(t)})\|_2 \quad (70\text{b})$$
$$\leq \|\mathbf{F}_i\|_2 \|\mathbf{Y}\|_{\mathrm{F}}, \quad (70\text{c})$$

where (70a) comes from the Cauchy-Schwartz inequality, (70b) from the constraint of problem (3), and (70c) from the definition of the operator norm. Moreover, by definition, the matrix ℓ_2-norm $\|\mathbf{F}_i\|_2$ is equal to the largest singular value of matrix $\mathbf{F}_i$, which is denoted by $\sigma_{\max}(\mathbf{F}_i)$. Inequality (70) holds for any solution with $\mathbf{Z} = \mathbf{0}$. Consequently, comparing (70) with (27b) yields the following result. Define

$$\lambda_{\max} = \|\mathbf{Y}\|_{\mathrm{F}} \cdot \max_{i=1,\dots,I} \{\sigma_{\max}(\mathbf{F}_i)\}.$$

For $\lambda \geq \lambda_{\max}$, any point $(\mathbf{D}, \mathbf{0})$ with $\mathbf{D} \in \mathcal{D}$ satisfies the conditions (27) and, hence, is stationary for $\widehat{h}^{(t)}$ in the domain of problem (3). We remark that $\lambda_{\max}$ above does not depend on the point $(\mathbf{D}^{(t)}, \mathbf{Z}^{(t)})$ where the majorization is made. Therefore, $(\mathbf{D}, \mathbf{0})$ is stationary for $\widehat{h}^{(t)}$ taken at any point, including $(\mathbf{D}, \mathbf{0})$. That means, it is also a stationary point of the original problem (3). Moreover, it is easy to verify that all points $(\mathbf{D}, \mathbf{0})$ with $\mathbf{D} \in \mathcal{D}$ are equally optimal for both $\widehat{h}^{(t)}$ and h. In conclusion, for $\lambda \geq \lambda_{\max}$, any point $(\mathbf{D}, \mathbf{0})$ is stationary for problem (3) and equally optimal.

In addition, $\lambda_{\max}$ can be further decreased in the investigated Case 1 and 2 in Section VI, where the linear operator $\mathcal{F}$ is given by (51). From the vectorized form in (63), we have

$$\mathbf{F}_i = \mathbf{b}_{i:} \otimes \mathbf{A}, \quad (71)$$

and $\mathbf{F}_i^{\mathrm{H}} \mathrm{vec}(\mathbf{Y}^{(t)}) = (\mathbf{b}_{i:} \otimes \mathbf{A})^{\mathrm{H}} \mathrm{vec}(\mathbf{Y}^{(t)}) = \mathbf{A}^{\mathrm{H}} \mathbf{Y}^{(t)} \bar{\mathbf{b}}_{i:}$. Then, directly substituting $\mathbf{F}_i$ in (71) into (70c), we obtain

$$|\nabla_{z_{pi}} \widehat{f}^{(t)}(\mathbf{D}, \mathbf{0})| \leq \|\mathbf{A}\|_2 \|\mathbf{b}_{i:}\|_2 \|\mathbf{Y}\|_{\mathrm{F}}. \quad (72)$$

On the other hand, exploiting the structure of $\mathbf{F}_i$ in (71), we can further derive the following inequality from (70b):

$$|\nabla_{z_{pi}}\widehat{f}^{(t)}(\mathbf{D},\mathbf{0})|\leq\|\mathbf{A}^{\mathrm{H}}\mathbf{Y}^{(t)}\bar{\mathbf{b}}_{i:}\|_2\leq\|\mathbf{A}\|_2\|\mathbf{Y}^{(t)}\bar{\mathbf{b}}_{i:}\|_2$$

$$=\|\mathbf{A}\|_2\Big\|\sum_{m=1}^{M_2}\bar{b}_{im}\mathbf{y}_m^{(t)}\Big\|_2\leq\|\mathbf{A}\|_2\sum_{m=1}^{M_2}|b_{im}|\cdot\|\mathbf{y}_m\|_2. \quad (73)$$

It is shown by Cauchy-Schwartz inequality that (73) is a tighter bound for $\nabla_{z_{pi}}\widehat{f}^{(t)}$ than (72). Consequently, in the case with $\mathcal{F}(\mathbf{X})=\mathbf{A}\mathbf{X}\mathbf{B}$, the upper bound $\lambda_{\max}$ can be decreased to

$$\lambda_{\max}=\sigma_{\max}(\mathbf{A})\cdot\max_{i=1,...,I}\Big\{\sum_{m=1}^{M_2}|b_{im}|\cdot\|\mathbf{y}_m\|_2\Big\}.$$

Furthermore, in Case 3 in Section VI, where spatial mixing is time-variant and temporal mixing is not applied, we have $\mathbf{F}_i=\mathbf{e}_i\otimes\mathbf{A}_i$ from the vectorized form in (78). Therefore, following the same procedure as in (73), we obtain the following bound for $\nabla_{z_{pi}}\widehat{f}^{(t)}$ tighter than (70c): $|\nabla_{z_{pi}}\widehat{f}^{(t)}(\mathbf{D},\mathbf{0})|\leq\|\mathbf{A}_i\|_2\|\mathbf{y}_i\|_2$. Consequently, in Case 3, $\lambda_{\max}$ can be refined to

$$\lambda_{\max}=\max_{i=1,...,I}\{\sigma_{\max}(\mathbf{A}_i)\cdot\|\mathbf{y}_i\|_2\}.$$

APPENDIX E
DERIVATION OF UPPER BOUND $\rho_{\max}$

We derive the upper bound $\rho_{\max}$ for the sparsity parameter ρ in (4) using the stationarity conditions (41)-(42). The gradients of $\widehat{f}^{(t)}$ are given in (32). Condition (41a) is trivial for $\mathbf{Z}=\mathbf{0}$ as $\nabla_{\mathbf{D}}\widehat{f}^{(t)}(\mathbf{X},\mathbf{D},\mathbf{0})=\mathbf{0}$ for any $\mathbf{X}$ and $\mathbf{D}$. Then, we have

$$|\nabla_{z_{pi}}\widehat{f}^{(t)}(\mathbf{X},\mathbf{D},\mathbf{0})|=\mu|\mathbf{d}_p^{\mathrm{H}}\mathbf{x}_i|\leq\mu\|\mathbf{d}_p\|_2\|\mathbf{x}_i\|_2\leq\mu\|\mathbf{x}_i\|_2 \quad (74)$$

for condition (41b). On the other hand, an upper bound for $\|\mathbf{x}_i\|_2$ can be derived from the vectorized form (57) of condition (42). When $\mathbf{Z}=\mathbf{0}$, condition (57) reduces to

$$\mathrm{vec}(\mathbf{X})=(\mathbf{F}^{\mathrm{H}}\mathbf{F}+\mu\mathbf{I}_{NI})^{-1}\mathbf{F}^{\mathrm{H}}\mathrm{vec}(\mathbf{Y}^{(t)}). \quad (75)$$

Therefore, the following upper bound for $\|\mathbf{x}_i\|_2$ is obtained:

$$\|\mathbf{x}_i\|_2\leq\|\mathbf{X}\|_{\mathrm{F}}\leq\|(\mathbf{F}^{\mathrm{H}}\mathbf{F}+\mu\mathbf{I}_{NI})^{-1}\|_2\|\mathbf{F}\|_2\|\mathbf{Y}\|_{\mathrm{F}}. \quad (76)$$

As an oversampling measurement operator $\mathcal{F}$ is considered, i.e., $M_1\geq N$ and $M_2\geq I$, we have $\|(\mathbf{F}^{\mathrm{H}}\mathbf{F}+\mu\mathbf{I}_{NI})^{-1}\|_2=\left(\sigma_{\min}^2(\mathbf{F})+\mu\right)^{-1}$. Consequently, combining (74) and (76) yields the following result. Define

$$\rho_{\max}=\frac{\mu\cdot\sigma_{\max}(\mathbf{F})\cdot\|\mathbf{Y}\|_{\mathrm{F}}}{\sigma_{\min}^2(\mathbf{F})+\mu}. \quad (77)$$

For $\rho\geq\rho_{\max}$, there always exists a feasible point $(\mathbf{X},\mathbf{D},\mathbf{0})$ that satisfies the stationarity conditions (41) and (42), and is, therefore, stationary for the majorizing function $\widehat{h}^{(t)}$. As $\rho_{\max}$ does not depend on the point $(\mathbf{X}^{(t)},\mathbf{D}^{(t)},\mathbf{Z}^{(t)})$ where the majorization is made, following the same line of arguments as in Appendix D, we further conclude that, for any $\rho\geq\rho_{\max}$, the original problem (4) admits a stationary point with $\mathbf{Z}=\mathbf{0}$.

In the investigated Case 1 and 3 in Section VI, where temporal mixing is not applied, the linear operator $\mathcal{F}$ and the corresponding matrix $\mathbf{F}$ can be expressed as

$$\mathcal{F}(\mathbf{X})=\sum_{i=1}^{I}\mathbf{A}_i\mathbf{X}\mathbf{B}_i \quad \text{and} \quad \mathbf{F}=\sum_{i=1}^{I}\mathbf{B}_i^{\mathrm{T}}\otimes\mathbf{A}_i, \quad (78)$$

where $\mathbf{B}_i=[\mathbf{0},...,\mathbf{0},\mathbf{e}_i,\mathbf{0},...,\mathbf{0}]$ only selects the i-th snapshot $\mathbf{x}_i$ and $\mathbf{A}_i$ is the spatial mixing designed for $\mathbf{x}_i$. Note that, in Case 1, where the spatial mixing is time-invariant, all matrices $\mathbf{A}_i$

are simply set to be the same value $\mathbf{A}$. Directly substituting $\mathbf{F}$ in (78) into (77), we obtain

$$\rho_{\max}=\frac{\mu\cdot\max_{i=1,...,I}\{\sigma_{\max}(\mathbf{A}_i)\}}{\min_{i=1,...,I}\{\sigma_{\min}^2(\mathbf{A}_i)\}+\mu}\cdot\|\mathbf{Y}\|_{\mathrm{F}}. \quad (79)$$

However, the upper bound $\rho_{\max}$ can be further decreased considering that each snapshot $\mathbf{x}_i$ is observed independently when temporal mixing is not applied. Using the matrix $\mathbf{F}$ in (78), we can reformulate the stationary condition (75) as

$$\mathbf{x}_i=(\mathbf{A}_i^{\mathrm{H}}\mathbf{A}_i+\mu\mathbf{I}_N)^{-1}\mathbf{A}_i^{\mathrm{H}}\mathbf{y}_i^{(t)}, \quad \text{for } i=1,...,I.$$

This results in a more refined bound of $\|\mathbf{x}_i\|_2$ than (76):

$$\|\mathbf{x}_i\|_2\leq\|(\mathbf{A}_i^{\mathrm{H}}\mathbf{A}_i+\mu\mathbf{I}_N)^{-1}\|_2\|\mathbf{A}_i\|_2\|\mathbf{y}_i^{(t)}\|_2.$$

Therefore, in Case 1 and 3, where temporal mixing is not applied, the upper bound $\rho_{\max}$ can be decreased to

$$\rho_{\max}=\max_{i=1,...,I}\Big\{\frac{\mu\sigma_{\max}(\mathbf{A}_i)}{\sigma_{\min}^2(\mathbf{A}_i)+\mu}\cdot\|\mathbf{y}_i\|_2\Big\}.$$

REFERENCES

[1] T. Liu, A. M. Tillmann, Y. Yang, Y. C. Eldar, and M. Pesavento, "A parallel algorithm for phase retrieval with dictionary learning," in *2021 IEEE Int. Conf. Acoust., Speech, Signal Process. (ICASSP)*, Jun. 2021, pp. 5619–5623.

[2] E. J. Candès, X. Li, and M. Soltanolkotabi, "Phase retrieval from coded diffraction patterns," *Appl. Comput. Harmon. Anal.*, vol. 39, no. 2, pp. 277–299, 2015.

[3] Y. Shechtman, Y. C. Eldar, O. Cohen, H. N. Chapman, J. Miao, and M. Segev, "Phase retrieval with application to optical imaging: A contemporary overview," *IEEE Signal Process. Mag.*, vol. 32, no. 3, pp. 87–109, May 2015.

[4] J. R. Fienup, "Phase retrieval algorithms: a comparison," *Appl. Opt., AO*, vol. 21, no. 15, pp. 2758–2769, Aug. 1982.

[5] R. W. Harrison, "Phase problem in crystallography," *J. Opt. Soc. Am. A, JOSAA*, vol. 10, no. 5, pp. 1046–1055, May 1993.

[6] H. Kim, A. M. Haimovich, and Y. C. Eldar, "Non-coherent direction of arrival estimation from magnitude-only measurements," *IEEE Signal Process. Lett.*, vol. 22, no. 7, pp. 925–929, 2014.

[7] R. W. Gerchberg and W. O. Saxton, "A practical algorithm for the determination of phase from image and diffraction plane pictures," *Optik*, vol. 35, pp. 237–246, 1972.

[8] E. J. Candès, X. Li, and M. Soltanolkotabi, "Phase retrieval via Wirtinger flow: Theory and algorithms," *IEEE Trans. Inf. Theory*, vol. 61, no. 4, pp. 1985–2007, Apr. 2015.

[9] G. Wang, G. B. Giannakis, and Y. C. Eldar, "Solving systems of random quadratic equations via truncated amplitude flow," *IEEE Trans. Inf. Theory*, vol. 64, no. 2, pp. 773–794, Feb. 2018.

[10] Y. Chen, Y. Chi, J. Fan, and C. Ma, "Gradient descent with random initialization: fast global convergence for nonconvex phase retrieval," *Math. Program.*, vol. 176, no. 1, pp. 5–37, Jul. 2019.

[11] Z. Wen, C. Yang, X. Liu, and S. Marchesini, "Alternating direction methods for classical and ptychographic phase retrieval," *Inverse Problems*, vol. 28, no. 11, p. 115010, Oct. 2012.

[12] J. Liang, P. Stoica, Y. Jing, and J. Li, "Phase retrieval via the alternating direction method of multipliers," *IEEE Signal Process. Lett.*, vol. 25, no. 1, pp. 5–9, 2017.

[13] E. J. Candès, T. Strohmer, and V. Voroninski, "Phaselift: Exact and stable signal recovery from magnitude measurements via convex programming," *Commun. Pure Appl. Math.*, vol. 66, no. 8, pp. 1241–1274, 2013.

[14] E. J. Candès, Y. C. Eldar, T. Strohmer, and V. Voroninski, "Phase retrieval via matrix completion," *SIAM Rev.*, vol. 57, no. 2, pp. 225–251, 2015.

[15] I. Waldspurger, A. d'Aspremont, and S. Mallat, "Phase recovery, maxcut and complex semidefinite programming," *Math. Program.*, vol. 149, no. 1, pp. 47–81, Feb. 2015.

[16] K. Jaganathan, Y. C. Eldar, and B. Hassibi, "STFT phase retrieval: Uniqueness guarantees and recovery algorithms," *IEEE J. Sel. Top. Signal Process.*, vol. 10, no. 4, pp. 770–781, Jun. 2016.

[17] T. Goldstein and C. Studer, "Phasemax: Convex phase retrieval via basis pursuit," *IEEE Trans. Inf. Theory*, vol. 64, no. 4, pp. 2675–2689, Apr. 2018.

[18] B. Wang, J. Fang, H. Duan, and H. Li, "Phaseequal: Convex phase retrieval via alternating direction method of multipliers," *IEEE Trans. Signal Process.*, vol. 68, pp. 1274–1285, 2020.

[19] A. Fannjiang and T. Strohmer, "The numerics of phase retrieval," *Acta Numer.*, vol. 29, pp. 125–228, May 2020.

[20] Y. C. Eldar, N. Hammen, and D. G. Mixon, "Recent advances in phase retrieval [lecture notes]," *IEEE Signal Process. Mag.*, vol. 33, no. 5, pp. 158–162, Sep. 2016.

[21] Y. Shechtman, A. Beck, and Y. C. Eldar, "Gespar: Efficient phase retrieval of sparse signals," *IEEE Trans. Signal Process.*, vol. 62, no. 4, pp. 928–938, Feb. 2014.

[22] Y. C. Eldar, P. Sidorenko, D. G. Mixon, S. Barel, and O. Cohen, "Sparse phase retrieval from short-time Fourier measurements," *IEEE Signal Process. Lett.*, vol. 22, no. 5, pp. 638–642, 2014.

[23] T. Qiu and D. P. Palomar, "Undersampled sparse phase retrieval via majorization–minimization," *IEEE Trans. Signal Process.*, vol. 65, no. 22, pp. 5957–5969, Nov. 2017.

[24] G. Wang, L. Zhang, G. B. Giannakis, M. Akçakaya, and J. Chen, "Sparse phase retrieval via truncated amplitude flow," *IEEE Trans. Signal Process.*, vol. 66, no. 2, pp. 479–491, Jan. 2018.

[25] E. J. R. Pauwels, A. Beck, Y. C. Eldar, and S. Sabach, "On Fienup methods for sparse phase retrieval," *IEEE Trans. Signal Process.*, vol. 66, no. 4, pp. 982–991, Feb. 2018.

[26] F. Salehi, E. Abbasi, and B. Hassibi, "Learning without the phase: Regularized phasemax achieves optimal sample complexity," in *Advances in neural information processing systems*, S. Bengio, H. Wallach, H. Larochelle, K. Grauman, N. Cesa-Bianchi, and R. Garnett, Eds., vol. 31. Curran Associates, Inc., 2018.

[27] Y. Yang, M. Pesavento, Y. C. Eldar, and B. Ottersten, "Parallel coordinate descent algorithms for sparse phase retrieval," in *2019 IEEE Int. Conf. Acoust., Speech, Signal Process. (ICASSP)*, May 2019, pp. 7670–7674.

[28] A. M. Tillmann, Y. C. Eldar, and J. Mairal, "DOLPHIn—dictionary learning for phase retrieval," *IEEE Trans. Signal Process.*, vol. 64, no. 24, pp. 6485–6500, Dec. 2016.

[29] Y. Yang and M. Pesavento, "A unified successive pseudoconvex approximation framework," *IEEE Trans. Signal Process.*, vol. 65, no. 13, pp. 3313–3328, 2017.

[30] M. R. Spiegel, S. Lipschutz, J. J. Schiller, and D. Spellman, *Complex variables*, 2nd ed. The McGraw-Hill Companies, 2009.

[31] Y. Yang, M. Pesavento, Z.-Q. Luo, and B. Ottersten, "Inexact block coordinate descent algorithms for nonsmooth nonconvex optimization," *IEEE Trans. Signal Process.*, vol. 68, pp. 947–961, 2020.

[32] Y. Sun, P. Babu, and D. P. Palomar, "Majorization-minimization algorithms in signal processing, communications, and machine learning," *IEEE Trans. Signal Process.*, vol. 65, no. 3, pp. 794–816, 2017.

[33] M. A. T. Figueiredo, R. D. Nowak, and S. J. Wright, "Gradient projection for sparse reconstruction: Application to compressed sensing and other inverse problems," *IEEE J. Sel. Top. Signal Process.*, vol. 1, no. 4, pp. 586–597, Dec. 2007.

[34] D. R. Hunter and K. Lange, "A tutorial on MM algorithms," *The American Statistician*, vol. 58, no. 1, pp. 30–37, Feb. 2004.

[35] S. Boyd and L. Vandenberghe, *Convex optimization*. Cambridge University Press, 2004.

[36] J. R. Bunch, C. P. Nielsen, and D. C. Sorensen, "Rank-one modification of the symmetric eigenproblem," *Numer. Math*, vol. 31, pp. 31–48, 1978.

[37] R.-C. Li, "Solving secular equations stably and efficiently," EECS Department, University of California, Berkeley, Tech. Rep. UCB/CSD-94-851, 1993.

[38] G. H. Golub and C. F. Van Loan, *Matrix Computations*, 4th ed. The Johns Hopkins University Press, 2013.

[39] R. Tibshirani, "Regression shrinkage and selection via the lasso," *R. Stat. Soc.*, vol. 58, no. 1, pp. 267–288, 1996.

[40] T. Liu, M. T. Hoang, Y. Yang, and M. Pesavento, "A block coordinate descent algorithm for sparse Gaussian graphical model inference with Laplacian constraints," in *2019 IEEE 8th Int. Workshop Comput. Advances Multi-Sensor Adaptive Process. (CAMSAP)*, Dec. 2019, pp. 236–240.

[41] D. L. Donoho, "De-noising by soft-thresholding," *IEEE Trans. Inf. Theory*, vol. 41, no. 3, pp. 613–627, May 1995.

[42] J. Li, A. M.-C. So, and W.-K. Ma, "Understanding notions of stationarity in nonsmooth optimization: A guided tour of various constructions of subdifferential for nonsmooth functions," *IEEE Signal Process. Mag.*, vol. 37, no. 5, pp. 18–31, Sep. 2020.

[43] F. H. Clarke, *Optimization and Nonsmooth Analysis*, ser. Classics in Applied Mathematics. Society for Industrial and Applied Mathematics, Jan. 1990.

[44] M. Razaviyayn, M. Hong, and Z.-Q. Luo, "A unified convergence analysis of block successive minimization methods for nonsmooth optimization," *SIAM J. Optim.*, vol. 23, no. 2, pp. 1126–1153, Jan. 2013.

[45] Y. Yang, M. Pesavento, S. Chatzinotas, and B. Ottersten, "Successive convex approximation algorithms for sparse signal estimation with nonconvex regularizations," *IEEE J. Sel. Top. Signal Process.*, vol. 12, no. 6, pp. 1286–1302, 2018.

[46] C. D. Manning, P. Raghavan, and H. Schütze, *Introduction to information retrieval*. New York: Cambridge University Press, 2008.

[47] S.-J. Kim, K. Koh, M. Lustig, S. Boyd, and D. Gorinevsky, "An interior-point method for large-scale ℓ_1-regularized least squares," *IEEE J. Sel. Top. Signal Process.*, vol. 1, no. 4, pp. 606–617, Dec. 2007.